Analysis of seasonal terrestrial water storage variations in regional climate simulations over Europe

Article *in* Journal of Geophysical Research Atmospheres · November 2007

DOI: 10.1029/2006JD008338

CITATIONS
36

READS
94

4 authors, including:

Martin Hirschi
ETH Zurich
82 PUBLICATIONS **9,659** CITATIONS
SEE PROFILE

Sonia I Seneviratne
ETH Zurich
487 PUBLICATIONS **43,412** CITATIONS
SEE PROFILE

Stefan Hagemann
Helmholtz-Zentrum Hereon
259 PUBLICATIONS **29,773** CITATIONS
SEE PROFILE

Analysis of seasonal terrestrial water storage variations in regional climate simulations over Europe

Martin Hirschi,[1] Sonia I. Seneviratne,[1] Stefan Hagemann,[2] and Christoph Schär[1]

Received 12 December 2006; revised 4 May 2007; accepted 22 August 2007; published 30 November 2007.

[1] Land-surface processes play a major role in the climate system, and their validation is crucial to improve current climate models. Here we investigate the seasonal evolution of terrestrial water storage (TWS) (includes all water stored on land) in an ensemble of 30-year-long climate simulations from the PRUDENCE archive (9 regional and 2 global models), representing current and future climatic conditions. For validation purposes we employ a recently published basin-scale water-balance (BSWB) data set of diagnosed monthly TWS variations, where the term variations refers to monthly changes in TWS. The analysis is conducted in five large-scale European domains composed of major river basins. This analysis shows that the climatology of most models lies within the interannual variability of the BSWB data set in the investigated regions, but the different models sometimes display considerable discrepancies in the seasonal evolution of TWS. In particular, we find that all models suffer from a considerable underestimation of interannual TWS variability. The deviations of the individual models from the BSWB data set can be linked to biases in the hydrological fluxes (i.e., precipitation, runoff, evapotranspiration). The simulated future changes for the Intergovernmental Panel on Climate Change (IPCC) A2 scenario suggest an enhancement of the seasonal cycle of TWS, with drier soils in summer. Mainly in the Central European domain, several models show a reduction of the year-to-year variability of summer TWS variations, indicating an exhaustion of the models' soil water reservoirs by the end of summer under future climatic conditions.

Citation: Hirschi, M., S. I. Seneviratne, S. Hagemann, and C. Schär (2007), Analysis of seasonal terrestrial water storage variations in regional climate simulations over Europe, *J. Geophys. Res.*, *112*, D22109, doi:10.1029/2006JD008338.

1. Introduction

[2] All current climate models contain some description of land-surface processes embedded in a range of land-surface models (LSMs). The LSM is responsible for simulating the surface water and energy balance, i.e., it controls the partitioning of available water at the land surface between evapotranspiration and runoff as well as the partitioning of surface energy between the sensible and latent heat fluxes. While the first LSM implemented by *Manabe* [1969] used a simple bucket to represent the land-surface hydrology, more complex LSMs have been developed in the last few decades, in order to include further components and processes such as multilayer soils, vegetation, or explicitly modeled canopy conductance (for an overview on the different generations of LSMs, see *Pitman* [2003]).

[3] Terrestrial water storage (TWS) comprehends soil moisture, groundwater, snow, surface water, canopy interception and biomass water, and is a central element of the hydrological cycle of a climate model. In particular, both soil moisture and snow are important memory components of the climate system [e.g., *Delworth and Manabe*, 1988; *Koster and Suarez*, 2001; *Schär et al.*, 2004a; *Seneviratne et al.*, 2006a], and soil moisture-precipitation as well as soil moisture-temperature feedbacks appear relevant both for global and regional climate [e.g., *Eltahir*, 1998; *Schär et al.*, 1999; *Betts*, 2004; *Koster et al.*, 2004, 2006; *Seneviratne et al.*, 2006b; *Fischer et al.*, 2007]. An accurate representation of land-surface processes, in particular the ability to simulate present-day TWS evolution on continental to subcontinental scales, is therefore essential for predicting future changes in the hydrological cycle [e.g., *Allen and Ingram*, 2002], streamflow and water availability [e.g., *Milly et al.*, 2005], and related impacts on the occurrence of droughts [e.g., *Wetherald and Manabe*, 1999; *Seneviratne et al.*, 2002], heat waves [e.g., *Schär et al.*, 2004b; *Seneviratne et al.*, 2006b], or floods [e.g., *Milly et al.*, 2002; *Kleinn et al.*, 2005].

[4] However, dense measurement networks of TWS and its components are extremely scarce. Soil moisture is measured routinely only at a few locations around the world, mostly in the former Soviet Union, Mongolia, China, India, Illinois and Oklahoma [e.g., *Robock et al.*, 2000]. In situ snow and groundwater measurements are even more limited [e.g., *Rodell and Famiglietti*, 2001; *Seneviratne et al.*, 2004]. And the newly available, remotely sensed large-

[1] Institute for Atmospheric and Climate Science, ETH Zurich, Zurich, Switzerland.
[2] Max Planck Institute for Meteorology, Hamburg, Germany.

0148-0227/07/2006JD008338

scale variations in TWS from the Gravity Recovery and Climate Experiment (GRACE) [*Tapley et al.*, 2004; *Wahr et al.*, 2004] cannot yet provide decadal information on TWS variations for model validation. An alternative is to use basin-scale ($>10^5-10^6$ km^2) atmospheric-terrestrial water-balance estimates of TWS diagnosed with streamflow measurements and reanalysis data [*Seneviratne et al.*, 2004]. Here we use a recently created data set derived with this approach (basin-scale water-balance (BSWB) data set [*Hirschi et al.*, 2006]) for the validation of the seasonal variations of TWS in climate simulations.

[5] The main focus of the present study is the validation of an ensemble of climate models (9 regional climate models (RCMs), and 2 global climate models (GCMs)) involved in the EU project PRUDENCE (Prediction of Regional Scenarios and Uncertainties for Defining European Climate Change Risks and Effects; see http://prudence.dmi.dk/) with regards to TWS in five large-scale European domains. In addition, we also investigate other hydrological variables, in order to make links between biases in TWS and those in other components of the hydrological cycle. This investigation represents an extension of the PRUDENCE model-simulation analyses published in the special issue of Climatic Change [*Christensen et al.*, 2007].

[6] The paper is structured as follows. Section 2 gives an overview of the analyzed RCMs and describes the employed BSWB data set together with the additional validation data used for the analysis. Section 3 provides a brief introduction to the figures presented in the following sections and discusses some features of the overall models' behavior that are common for all domains. Section 4 presents the regional validation and analysis of the modeled seasonal TWS variations for the control period 1961–1990. A similar investigation for some individual models is provided in section 5. Additionally, the model biases and interrelated processes are analyzed in more depth in section 6. Simulated climate-change induced modifications of the seasonal cycle of TWS are presented in section 7. Finally, section 8 provides a further discussion of the results as well as the main conclusions.

2. Methods and Data

2.1. Analyzed Regional Climate Simulations

[7] The present analysis encompasses 9 RCMs, 1 GCM with a stretched grid, and 1 standard GCM involved in the EU project PRUDENCE [*Christensen et al.*, 2007]. The models differ with respect to the physical and dynamical formulations, land use characteristics and computational domains (see Tables 1 and 2). The regional climate simulations cover the major part of Europe at a resolution of approximately 50 km (0.44–0.5°). The RCMs simulate a control (1961–1990) and an A2 scenario climate (2071–2100), and are all driven by the same respective boundary conditions from the global model HadAM3H (1.875 × 1.25° resolution [*Pope et al.*, 2000]). In the control period, HadAM is driven by observed sea-surface temperatures (SSTs) and sea ice (SI) from the HadISST data set [*Rayner et al.*, 2003], and in the scenario period by a sea-surface forcing derived by adding the monthly SST/SI anomaly fields from the AOGCM HadCM3 A2 scenario run (with respect to its simulated control climatology) to the observed SST/SI climatology [*Christensen and Christensen*, 2007]. A slightly different setup is used for the high-resolution simulations of the global model ARPEGE (stretched grid with 0.5° resolution over Southern Europe). These simulations are directly forced with the same sea-surface conditions as HadAM.

[8] Here, we focus on the monthly TWS variations of the models (including soil water and snow water changes) as well as on a series of related processes (precipitation, evapotranspiration, runoff, net radiation and temperature). A more detailed analysis and validation of precipitation, evapotranspiration, runoff and temperature is given by *Hagemann and Jacob* [2007] and *Jacob et al.* [2007]. Note that for HadAM only the 30-year climatology (and not the full time series) of runoff and snow water changes were available (these variables were directly received from David Hein, Met Office, UK).

[9] Our analysis concentrates on the warm period of the year (spring to autumn) when TWS interacts actively with the other components of the hydrological cycle, whereas the European winter climate is predominately determined by larger-scale advective processes and the land surface is essentially decoupled from the atmospheric circulation [*Viterbo and Beljaars*, 2004]. Moreover, in Central Europe the dynamic boundary forcing of the regional models is strong in winter and thus the simulated circulation statistics are close to those of the driving model HadAM [*van Ulden et al.*, 2007]. This coupling is weaker in summer and the regional models can create their own climate more independently.

[10] In the first part of the study, the mean seasonal cycles of the investigated processes are analyzed using diagnosed and directly observed validation data (sections 3–5). In the second part, we look into the relations between the monthly model biases in these mean seasonal cycles (section 6.1), and relate them to the models' evapotranspiration, runoff and temperature regimes. Furthermore, we examine the interannual variability of the models and of the validation data by investigating lagged correlations between different variables (section 6.2). The last part briefly presents some aspects of the future TWS cycle under the A2 scenario (section 7).

2.2. TWS: Basin-Scale Water-Balance (BSWB) Data

[11] The diagnostic data set of monthly TWS variations used in this study was derived from combined atmospheric and terrestrial water-balance computations, using streamflow measurements and ERA-40 reanalysis data (see http://www.ecmwf.int/research/era). For a given river basin, the BSWB data set estimates monthly variations in TWS as

$$\left\{\frac{\overline{\partial S}}{\partial t}\right\} = -\left\{\frac{\overline{\partial W}}{\partial t}\right\} - \left\{\overline{\nabla_H \vec{Q}}\right\} - \{R\} \quad , \qquad (1)$$

where S represents the TWS of the area, W the column storage of atmospheric water vapor, $\vec{Q}$ the vertically integrated two-dimensional atmospheric water vapor flux and R the measured streamflow (assumed to include both the surface and the groundwater runoff of the area). The operator (∇_H) represents the horizontal divergence, the overbar a temporal average (i.e., monthly means) and {} a spatial average over the region. The spatial scale at which

Table 1. Overview of the Analyzed PRUDENCE Models

Model	Institute	Model Description	Reference
CHRM	ETH	adapted from the German Weather Service High-Resolution Model	*Vidale et al.* [2003]
RACMO	KNMI	RACMO2, dynamics taken from HIRLAM (version 5.0), physical parameterization from ECMWF (cycle 23R4 with increased soil storage capacity and convective triggering)	*Lenderink et al.* [2003]
HIRHAM	DMI	HIRHAM4, with HIRLAM dynamics and the ECHAM4 physical parameterization, with adjustments in the formation of low-intensity precipitation	*Christensen et al.* [1996]
CLM	GKSS	adapted from the German Weather Service Lokalmodell	*Steppeler et al.* [2003]
RCAO	SMHI	Rossby Centre regional Atmosphere-Ocean model, consisting of the atmospheric model RCA, the three-dimensional Baltic Sea ocean model RCO and the lake model PROBE. RCA is based on the HIRLAM system with a modified land surface parameterization.	*Döscher et al.* [2002]
REMO	MPI	dynamics as CHRM, but using the ECHAM physical parameterizations	*Jacob* [2001]
PROMES	UCM	hydrostatic and fully compressible atmospheric model, entirely developed at UCM	*Sanchez et al.* [2004]
ARPEGE	CNRM	ARPEGE-IFS, global operational forecast model used at ECMWF and the French Meteorological Service (stretched grid with 0.5° resolution over S-Europe), driven by observed SST/SI in control run and HadCM3 in scenario run (instead of HadAM3H; see below)	*Déqué et al.* [1998]
RegCM	ICTP	dynamics essentially equivalent to the hydrostatic version of the NCAR/Pennsylvania State University mesoscale model MM5	*Giorgi et al.* [1993a, 1993b]
HadRM	Hadley Centre	Hadley Centre regional climate model HadRM3H, limited area higher-resolution version of the AGCM HadAM3H	*Jones et al.* [2001]
HadAM	Hadley Centre	HadAM3H, driving model for the regional climate models described above, improved version of HadAM3, the atmospheric component of the Hadley Centre coupled AOGCM (HadCM3)	*Pope et al.* [2000]

Table 2. Characteristics of the Land-Surface Models of the Analyzed Models

Model	Land Surface Scheme	Soil Layers	Soil Depth
CHRM	TERRA, adapted from *Dickinson* [1984] and *Jacobsen and Heise* [1982]	3 moisture, 2 thermal	1.7 m
RACMO	TESSEL [*van den Hurk et al.*, 2000]	4 moisture, 4 thermal	5 m [*Lenderink et al.*, 2003] (originally 2.89 m)
HIRHAM	ECHAM4	1 moisture, 5 thermal	10 m for temperature, up to 4 m for water (spatially variable)
CLM	TERRA_LM [*Jacobsen and Heise*, 1982], multilayer version [*Schrodin and Heise*, 2001]	9 moisture, 9 thermal	2.5 m
RCAO	RCA2 [*Bringfelt et al.*, 2001]	2 moisture, 3 thermal	0.9 m
REMO	ECHAM4	1 moisture, 5 thermal	10 m for temperature, up to 4 m for water (spatially variable)
PROMES	SECHIBA [*Ducoudré et al.*, 1993]	2 moisture, 7 thermal	up to 2 m (depending on plant functional type)
ARPEGE	ISBA, improved standard configuration [*Douville et al.*, 2000]	4 thermal, 2 moisture	up to 4 m (depending on surface type [*Manzi and Planton*, 1994])
RegCM	BATS1e [*Dickinson et al.*, 1993]	3 moisture, 3 thermal	5 m
HadRM	MOSES [*Cox et al.*, 1999]	4 moisture, 4 thermal	3 m
HadAM	MOSES [*Cox et al.*, 1999]	4 moisture, 4 thermal	3 m

Table 3. Modeled Mean Annual TWS Amplitudes in the Various Domains Compared Against BSWB Data During the Control Period[a]

	Domains				
Model	Central Europe	Northeast Europe	France	Baltic Sea	Danube
CHRM	134	125	152	164	98
RACMO	152	142	194	98	117
HIRHAM	136	123	174	134	117
CLM	107	103	116	140	87
RCAO	126	123	143	87	134
REMO	130	126	158	93	141
PROMES	41	32	52	–	61
ARPEGE	115	101	134	160	136
RegCM	161	132	192	–	144
HadRM	117	88	131	66	97
ensemble mean RCMs	121	109	143	89	111
HadAM (driving model)	81	73	111	70	77
BSWB	95	96	142	111	133

[a]Amplitudes are in mm. Note the Baltic Sea catchment is not covered by PROMES and RegCM.

(1) can be applied is of the order of at least 10^5–10^6 km^2 [e.g., *Rasmusson*, 1968; *Seneviratne et al.*, 2004; *Hirschi et al.*, 2006].

[12] ERA-40 atmospheric reanalysis data was used for the terms $\left\{\overline{\partial W/\partial t}\right\}$ and $\left\{\overline{\nabla_H \vec{Q}}\right\}$, which are both constrained by assimilated radiosonde observations. For the term $\{\overline{R}\}$, we used conventional runoff data from the Global Runoff Data Centre (GRDC), from *Bergström and Carlsson* [1993] (in the Baltic Sea catchment) and from local sources (in the French domain). The temporally limited availability of runoff data in some river basins leads to a shortening of the analyzed control period (normally 1961–1990) in the Central European and French domains (1972–1990) as well as in the Baltic Sea catchment (1961–1989). The occurring time-dependent long-term drift in TWS, likely due to biases in atmospheric moisture convergence [e.g., *Seneviratne et al.*, 2004], is removed using a simple high-pass filter (by subtracting a running mean with 3-year window [see *Hirschi et al.*, 2006]). Amplitudes of the BSWB data (Table 3), i.e., $S_{\max}$-$S_{\min}$, were calculated using the mean seasonal cycles of the "absolute" values of TWS obtained with

$$S(t) = S_0 + \int_{t_0}^{t} \left\{\frac{\overline{\partial S}}{\partial t}\right\}_{filtered} \cdot dt \quad with\ S_0 = 0\ mm. \tag{2}$$

[13] The described approach was developed and first tested for the Mississippi River basin and Illinois [*Seneviratne et al.*, 2004]. It has subsequently been applied to presently 37 major midlatitude river basins in Europe, Asia, North America and Australia [*Hirschi et al.*, 2006]. The resulting BSWB data set covers the 44-year time period of the ERA-40 reanalysis but is temporally limited in some river basins depending on the availability of runoff data. Validation of the BSWB data set showed good agreement with in situ observations in Illinois (soil moisture, groundwater and snow observations [*Seneviratne et al.*, 2004]) and the former Soviet Union (soil moisture and snow observations [*Hirschi et al.*, 2006]). The BSWB data set is available for download at www.iac.ethz.ch/data/water_balance.

2.3. Evapotranspiration

[14] Due to lack of sufficient ground observations, a basin-scale atmospheric water-balance estimate is used for the analysis of evapotranspiration in the RCMs. It is diagnosed using the atmospheric water-balance equation, following which evapotranspiration for a given river basin can be expressed as

$$\{\overline{E}\} = \{\overline{P}\} + \left\{\frac{\overline{\partial W}}{\partial t}\right\} + \left\{\overline{\nabla_H \vec{Q}}\right\}, \tag{3}$$

where E represents the evapotranspiration of the area and P the precipitation. As for the BSWB data set, ERA-40 atmospheric reanalysis data is used for the terms $\left\{\overline{\partial W/\partial t}\right\}$ and $\left\{\overline{\nabla_H \vec{Q}}\right\}$, and observed precipitation from the Climate Research Unit (CRU) [*New et al.*, 1999, 2000] is used for the term $\{\overline{P}\}$. To correct for biases in the atmospheric moisture convergence (see previous section), the same drift correction as for the monthly TWS variations is applied for the diagnosed evapotranspiration. Note, however, that we do not correct for possible biases in observed precipitation, e.g., due to undercatch of solid precipitation by the rain gauges (CRU precipitation being not corrected for gauge biases). According to *Legates and Willmott* [1990], the underestimation of global-mean precipitation resulting from all systematic biases in the observational network might amount to about 11%. One should additionally remark that since the diagnosed TWS variations and evapotranspiration are based on the same ERA-40 data, these validation data sets are not strictly independent.

2.4. Other Data Sets

[15] Additional validation data sets used for the analysis include observed precipitation and temperature from the CRU [*New et al.*, 1999, 2000] as well as runoff measurements from local sources (French domain), from *Bergström and Carlsson* [1993] (Baltic Sea catchment), and from the GRDC (other domains). Moreover, simulated net radiation is assessed with ERA-15 radiation, which has shown good agreement with measurements from the Global Energy Balance Archive (GEBA) [*Gilgen and Ohmura*, 1999], a database of worldwide instrumentally-measured energy fluxes [*Wild et al.*, 1998].

2.5. Runoff Computation

[16] Since we mainly focus on the monthly variations in TWS in this paper, no river routing scheme is applied to the gridded runoff from the regional simulations when comparing it with downstream observed station runoff. Thus a part of the biases in nonrouted model runoff may result from a time delay in the measured runoff. Discharge computations with a simplified land surface scheme (SL) [*Hagemann and Dümenil*, 2003] and the Hydrological Discharge model (HD) [*Hagemann and Dümenil*, 2001] using precipitation, 2 m temperature and evapotranspiration from the same regional climate simulations as in the present study as forcing led to slightly differing annual discharge cycles in the Baltic Sea catchment and in the Danube basin [see

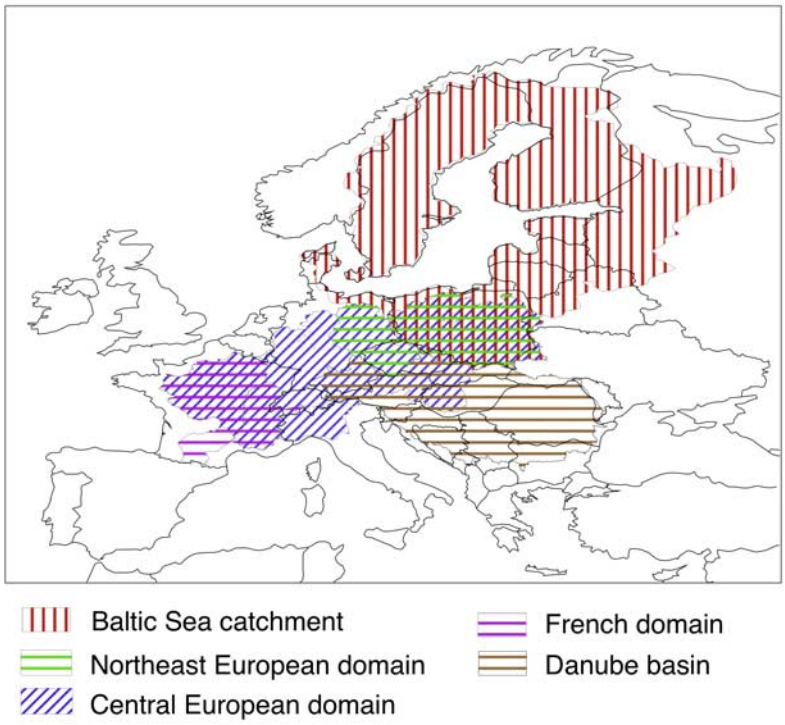

Figure 1. Analyzed European domains: Baltic Sea catchment, Northeast European domain (including the Wisla, Odra, and Elbe river basins), Central European domain (Wisla, Odra, Elbe, Weser, Rhine, Seine, Loire, Rhone, and Po river basins as well as northern parts of the Danube basin), French domain (Seine, Loire, Garonne, and Rhone river basins), and Danube river basin.

Hagemann and Jacob, 2007, Figure 8]. The spring peaks of most models were delayed by one to two months. Moreover, the overall spread of the models was smaller and the strong spring (snow melt) biases of some models were reduced.

[17] To test the effect of a delay in observed station runoff (compared to the basin average of gridded runoff) on the diagnosed BSWB data (section 2.2) and its comparison with the simulated TWS variations, the BSWB estimates were also calculated using the observed runoff of the subsequent month, instead of the simultaneously observed streamflow (i.e., assuming a time lag of one month, according to *Hagemann et al.* [2004]). This did not markedly change the agreement with the RCMs (see section 3.2).

[18] In addition, one has to keep in mind that human influences on the hydrological cycle (e.g., through irrigation or by constructing reservoirs and dams) can considerably alter the natural discharge curves in individual river basins [e.g., *van den Hurk et al.*, 2005; *Hanasaki et al.*, 2006; *Haddeland et al.*, 2006], but are not accounted for in the analyzed regional climate simulations. However, with regard to large-scale TWS variations as investigated here, simulations with a reservoir operating scheme for global river discharge models showed that continental-scale changes in reservoir storage were small in proportion to the total storage capacity [*Hanasaki et al.*, 2006].

2.6. Analyzed Domains

[19] The definition of the analyzed domains is determined by the availability of the diagnostic BSWB data, which itself depends on the availability of runoff observations, and by the spatial-scale requirement for the water-balance computations (see section 2.2). For the latter reason, smaller-scale river basins have been combined here to five large-scale European domains (Figure 1), which are partly based on those of precedent PRUDENCE analyses [e.g., *Hagemann and Jacob*, 2007; *Christensen and Christensen*, 2007]: the Central European (1 191 310 km^2), Northeast European (432 720 km^2), and French (335 450 km^2) domains as well as the Baltic Sea catchment (1 684 680 km^2) and the Danube (772 220 km^2) river basin. The Central European domain includes the Wisla, Odra, Elbe, Weser, Rhine, Seine, Loire, Rhone, Po and northern parts of the Danube river basins; the Northeast European domain comprises the Wisla, Odra and Elbe basins; and the French domain consists of the Seine, Loire, Rhone and Garonne basins. Note that the Baltic Sea catchment lies outside the PROMES and RegCM model domains.

3. Seasonal Cycle of Hydrological Variables: Analysis Approach and General Results

[20] In this and the following two sections we will present an analysis of Figures 2–10, which provide a broad investigation of the models in the selected domains. In this section, we will describe the content of the figures and discuss some features of the overall models' behavior common for the domains. An analysis for the individual regions and models is provided in sections 4 and 5, respectively.

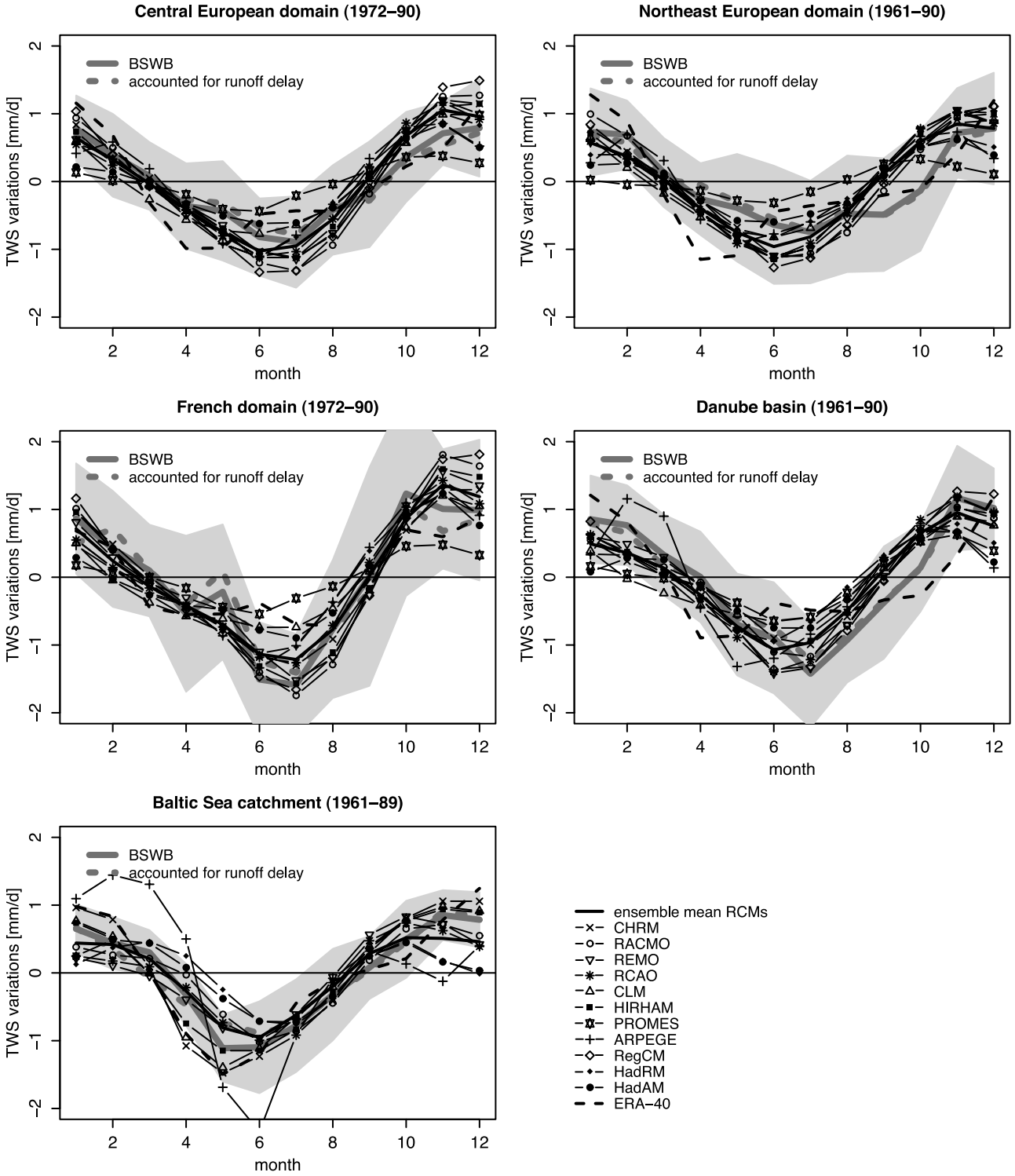

Figure 2. Modeled mean monthly TWS variations in the European domains compared against the diagnostic BSWB data: the 10 regional climate simulations and their ensemble mean as well as the global driving model (HadAM) and ERA-40 are shown. The shaded area denotes ± one monthly standard deviation of the BSWB data.

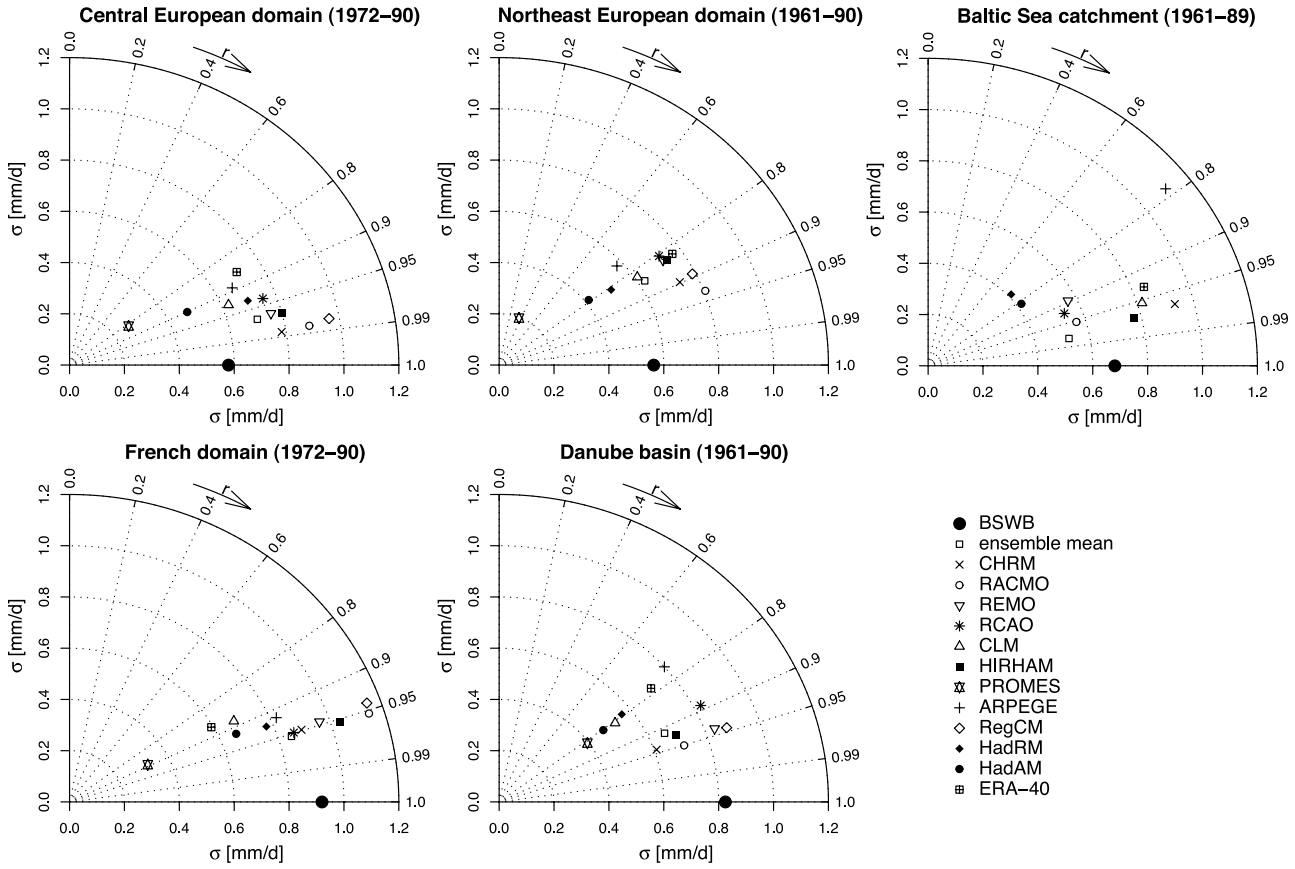

Figure 3. Taylor plots [*Taylor*, 2001] of the modeled mean seasonal cycles of TWS variations compared against the diagnostic BSWB data (standard deviation σ in mm/d and correlation coefficient r): the 10 regional climate simulations and their ensemble mean as well as the global driving model (HadAM) and ERA-40 are shown.

3.1. Analysis Approach and Figures' Content

[21] Figure 2 shows the mean seasonal cycles of the modeled monthly TWS variations (composed of simulated changes in soil moisture and snow water equivalent) of the control period compared with the BSWB data of monthly TWS variations (with shading areas denoting ± one monthly standard deviation σ). The 10 regional climate simulations (i.e., the 9 regional models and the stretched grid simulation of the global model ARPEGE) are displayed separately and as an ensemble mean. Also the global driving model HadAM is shown, and the raw ERA-40 TWS variations (i.e., the changes in soil water and snow water equivalent from the ERA-40 soil moisture and snow analysis) are plotted for comparison.

[22] Figure 3 presents Taylor plots [*Taylor*, 2001] for all domains, showing the standard deviations σ and the correlation coefficients r of the modeled mean seasonal cycles of TWS variations compared against the diagnostic BSWB estimates. Table 3 lists simulated and diagnosed mean annual TWS amplitudes. Figure 4 shows the monthly year-to-year variability (i.e., the monthly standard deviations σ) of the modeled TWS variations compared against the diagnostic BSWB data. The shaded areas denote the 95% confidence intervals calculated using bootstrap resampling (10,000 samples).

[23] Figure 5 displays the mean seasonal cycle of absolute TWS for the models and the diagnosed BSWB data. The absolute TWS values are calculated according to (2) for the BSWB data. As an appropriate reference level cannot objectively be defined, we choose the reference such that the yearly mean of each cycle equals zero. Subsequently we will refer to this data as mean monthly TWS. Likewise, the differences between simulated and diagnosed TWS data will be referred to as mean monthly TWS biases.

[24] Figures 6–9 show the mean seasonal cycles of the modeled monthly precipitation (compared against observed CRU precipitation), evapotranspiration (compared against basin-scale evapotranspiration derived from CRU precipitation; see section 2.2), runoff (compared against observations from the GRDC, from *Bergström and Carlsson* [1993] or from local sources; see section 2.2) and net radiation (compared against climatological ERA-15 net radiation), respectively. Figure 10 displays the mean seasonal evolution of the modeled 2 m temperature bias from observed CRU temperature. As Figures 2–5, Figures 6–10 also include the respective ERA-40 data for comparison.

3.2. Overall Models' Behavior

[25] The simulated mean seasonal cycles of TWS variations are mostly situated within the year-to-year variability

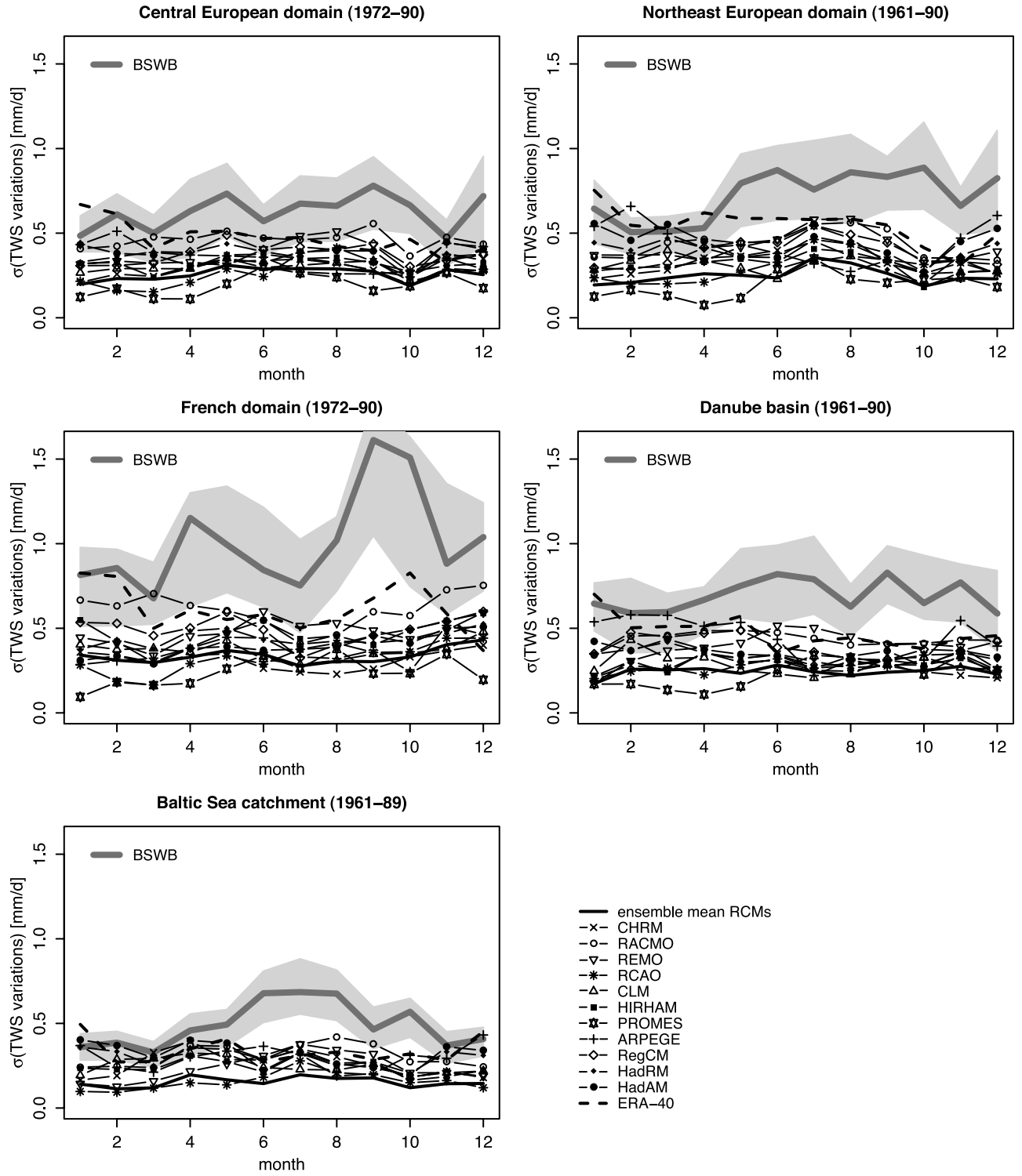

Figure 4. Monthly standard deviations σ of the modeled TWS variations in the European domains compared against the diagnostic BSWB data: the 10 regional climate simulations and their ensemble mean as well as the global driving model (HadAM) and ERA-40 are shown. The shaded areas denote the 95% confidence intervals calculated using bootstrap resampling (10,000 samples).

of the diagnostic BSWB data (denoted by the shaded area in Figure 2). However, the discrepancies between the individual models are sometimes considerable and can amount to more than 1 mm/d in the investigated domains in summer and winter. The mean seasonal cycle of monthly TWS variations of the ensemble mean of the RCMs is often closer to the BSWB data than most individual models (e.g., in terms of the standard deviation σ of the seasonal cycle;

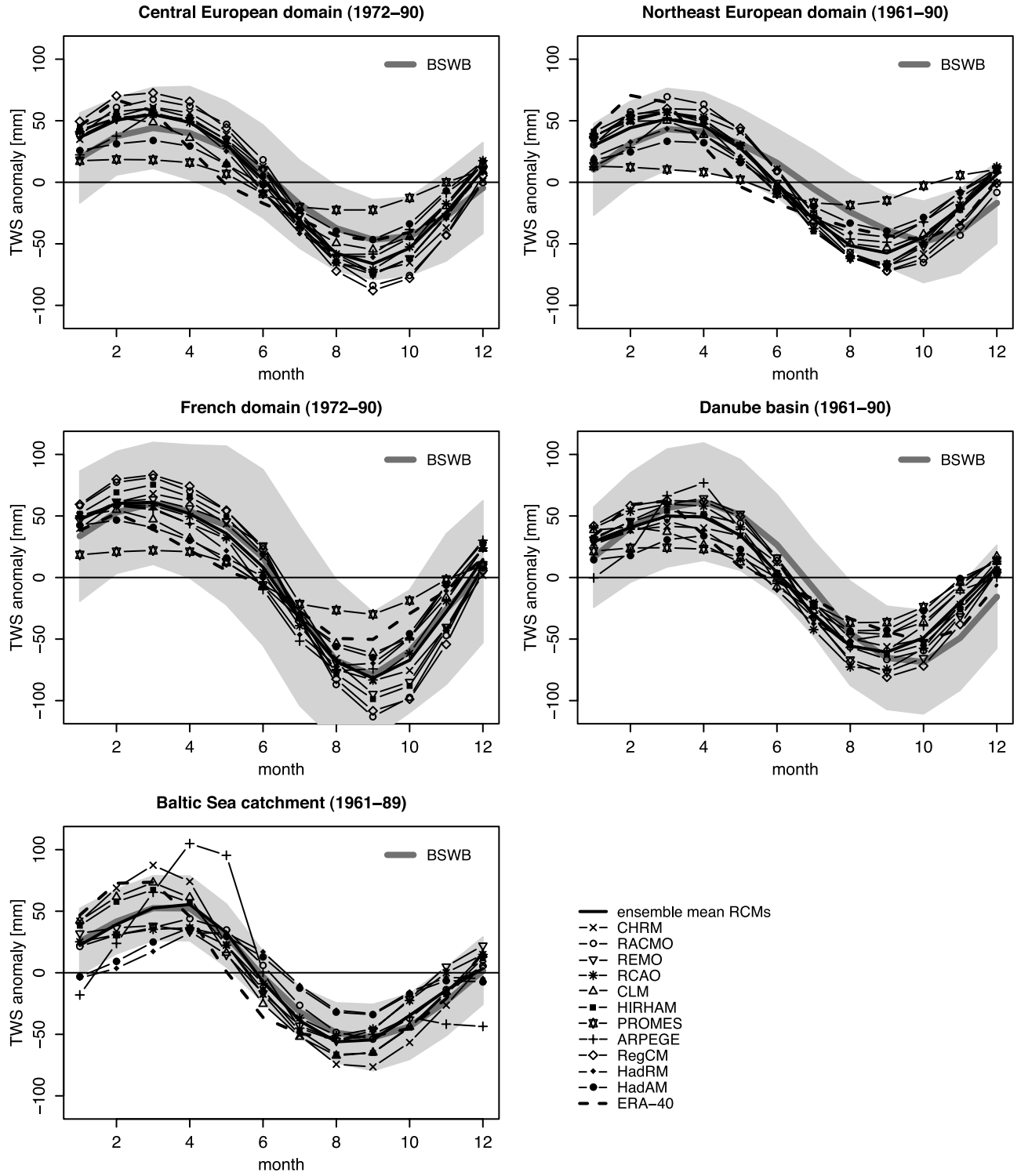

Figure 5. Same as Figure 2, but for the mean monthly absolute TWS. The yearly mean of each cycle is zero by design.

see Figure 3). Regarding the overall behavior of other simulated hydrological quantities, precipitation and evapotranspiration are generally overestimated in winter (except for precipitation in the Danube basin) and spring when compared to validation data (Figures 6 and 7). Since a slightly overestimated decrease in TWS is resulting for most simulations in spring (except in the Baltic Sea catchment; see Figure 2), the positive precipitation biases must be exceeded by the positive biases in evapotranspiration and partly runoff in this season. These are likely fed by excessive water storage resulting from overestimated autumn and winter precipitation. Moreover, model evapotranspiration is slightly underestimated in early autumn (except in the Baltic Sea catchment). Finally, the simulated

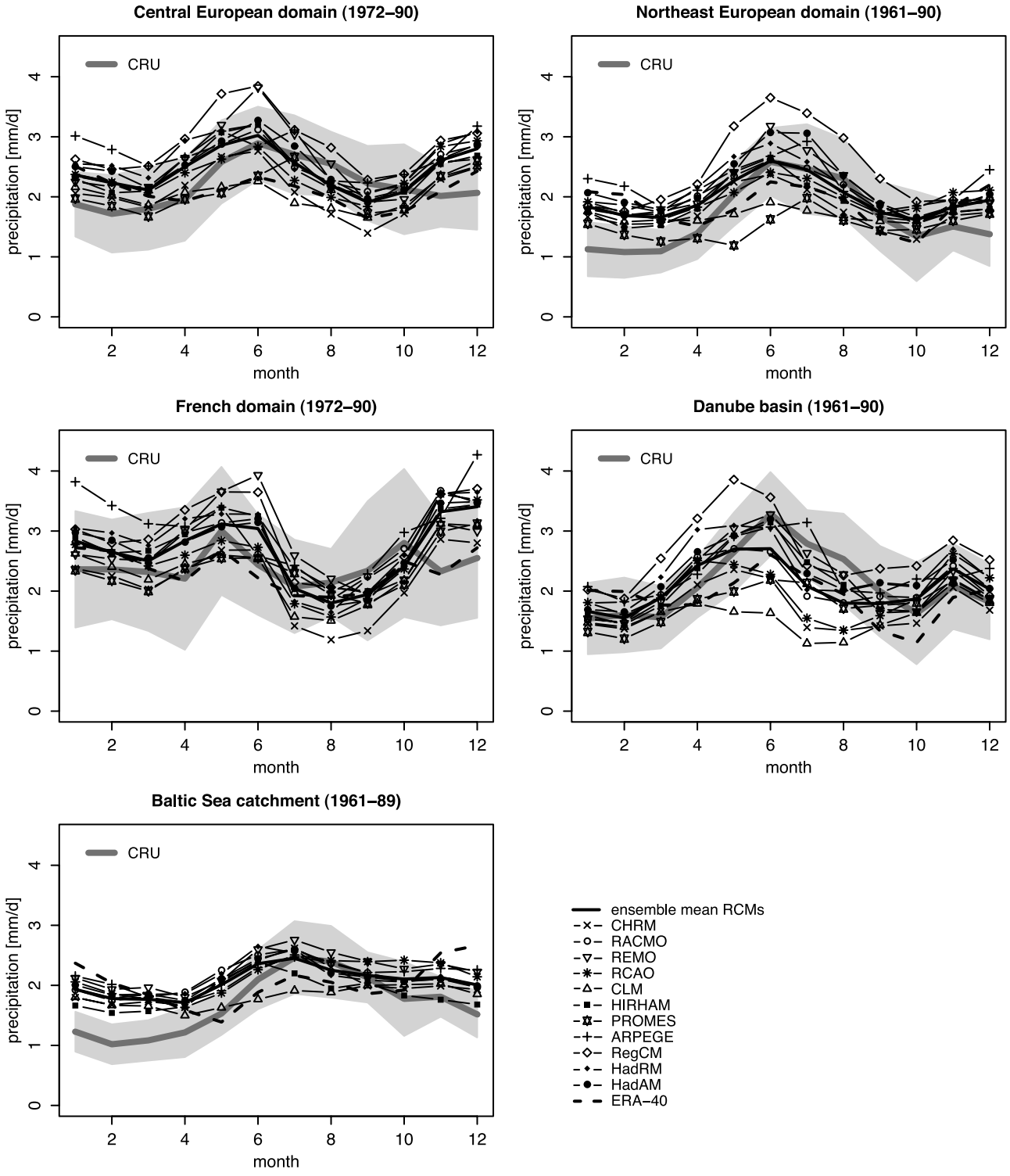

Figure 6. Same as Figure 2, but for precipitation (observations from CRU precipitation data set).

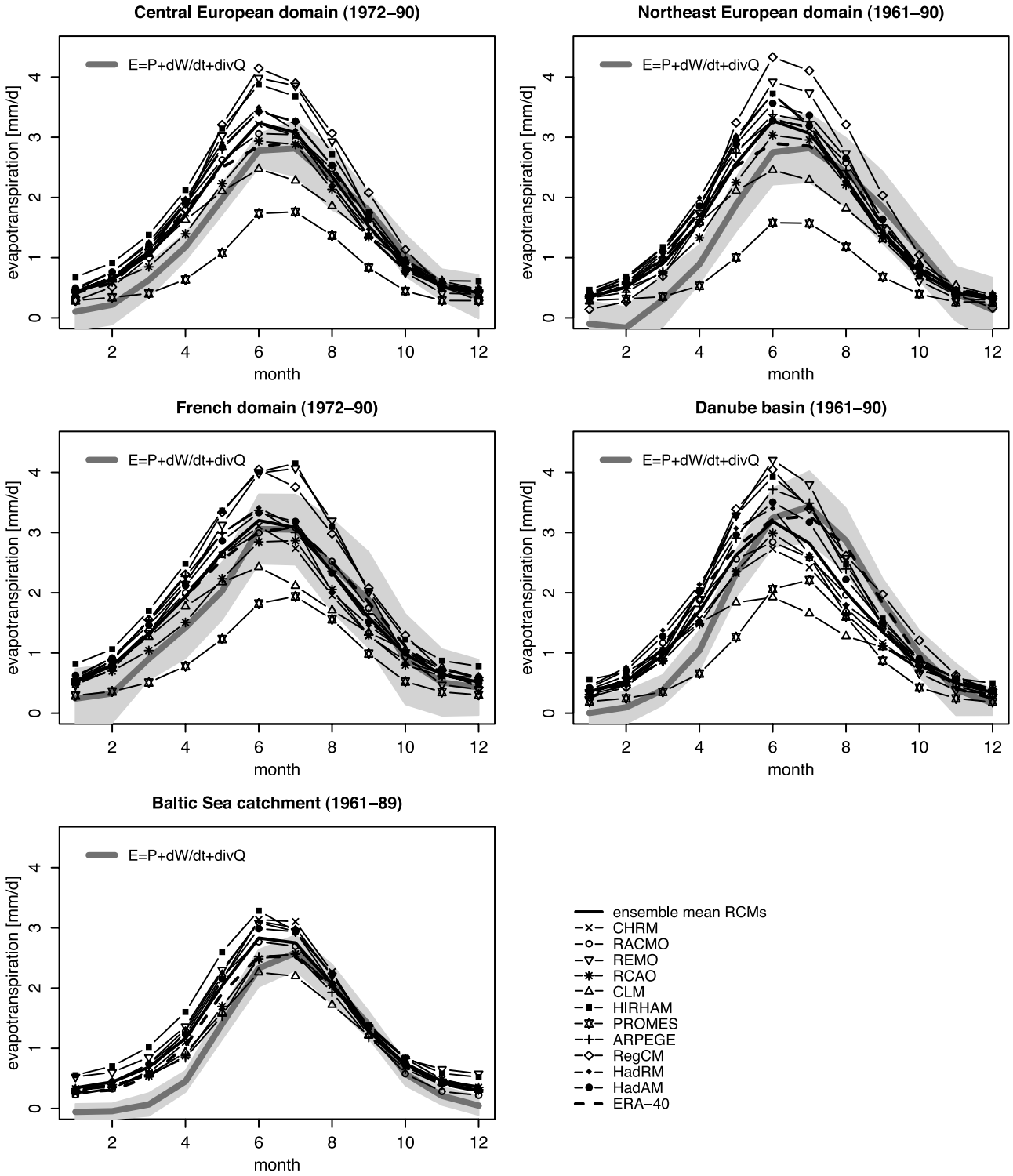

Figure 7. Same as Figure 2, but for evapotranspiration. The validation data is an atmospheric water-balance estimate based on ERA-40 convergence and observed CRU precipitation (see section 2.2). The slightly negative winter values in some domains are due to the neglect of the systematic rain gauge undercatch (see section 2.3).

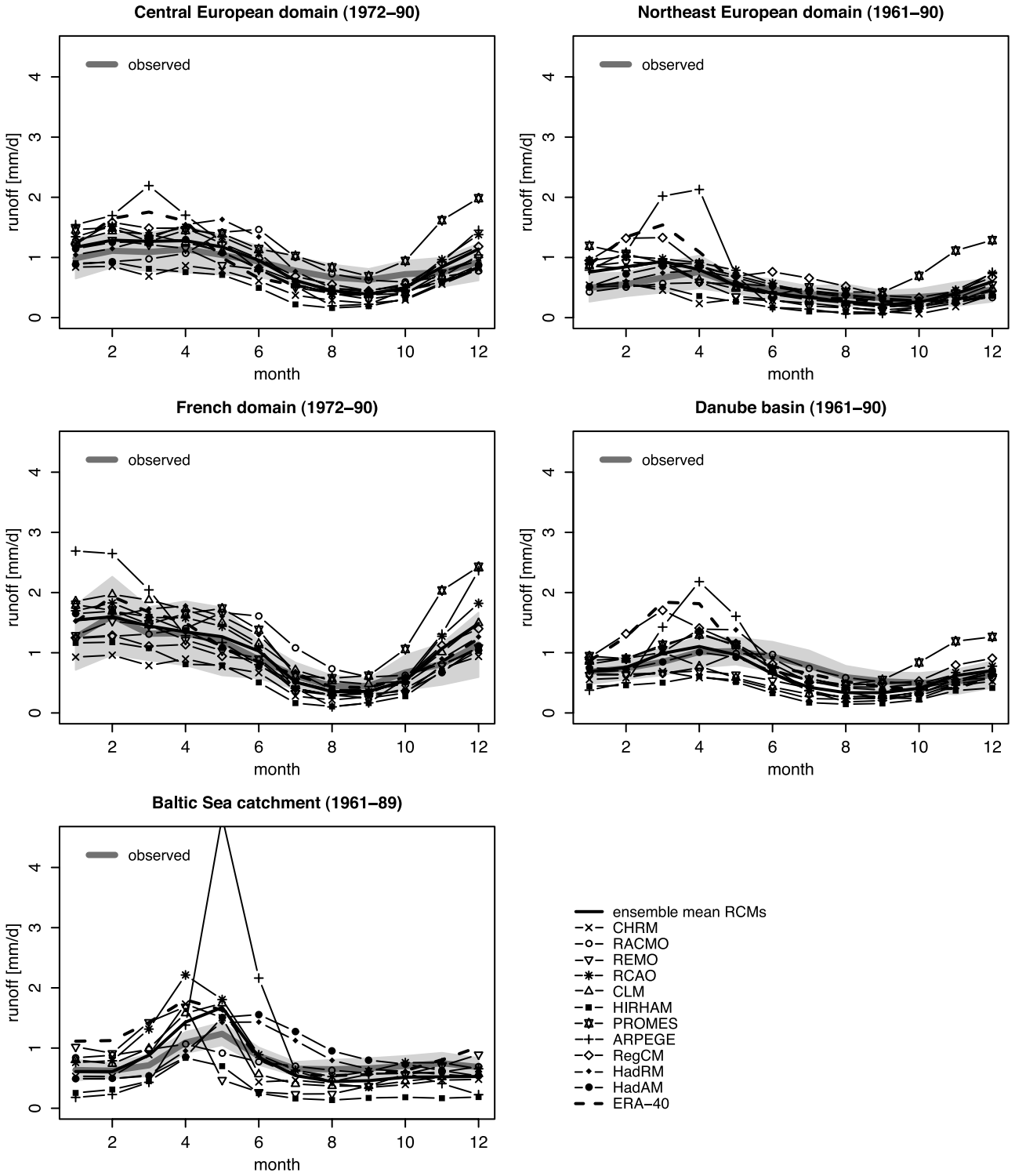

Figure 8. Same as Figure 2, but for runoff (observations from the GRDC, from *Bergström and Carlsson* [1993] and from local sources).

2 m temperatures show a general warm bias in summer (except in the French domain) and winter, and a cold bias in spring and autumn (Figure 10).

[26] The models generally exhibit a reduced interannual variability in monthly TWS variations, especially during summer (see Figure 4). The underestimation is largest in the French domain. A dominant fraction of the year-to-year summer variability of the BSWB data comes from the ERA-40 moisture flux convergence applied in the computation of the combined water balance (see section 2.2),

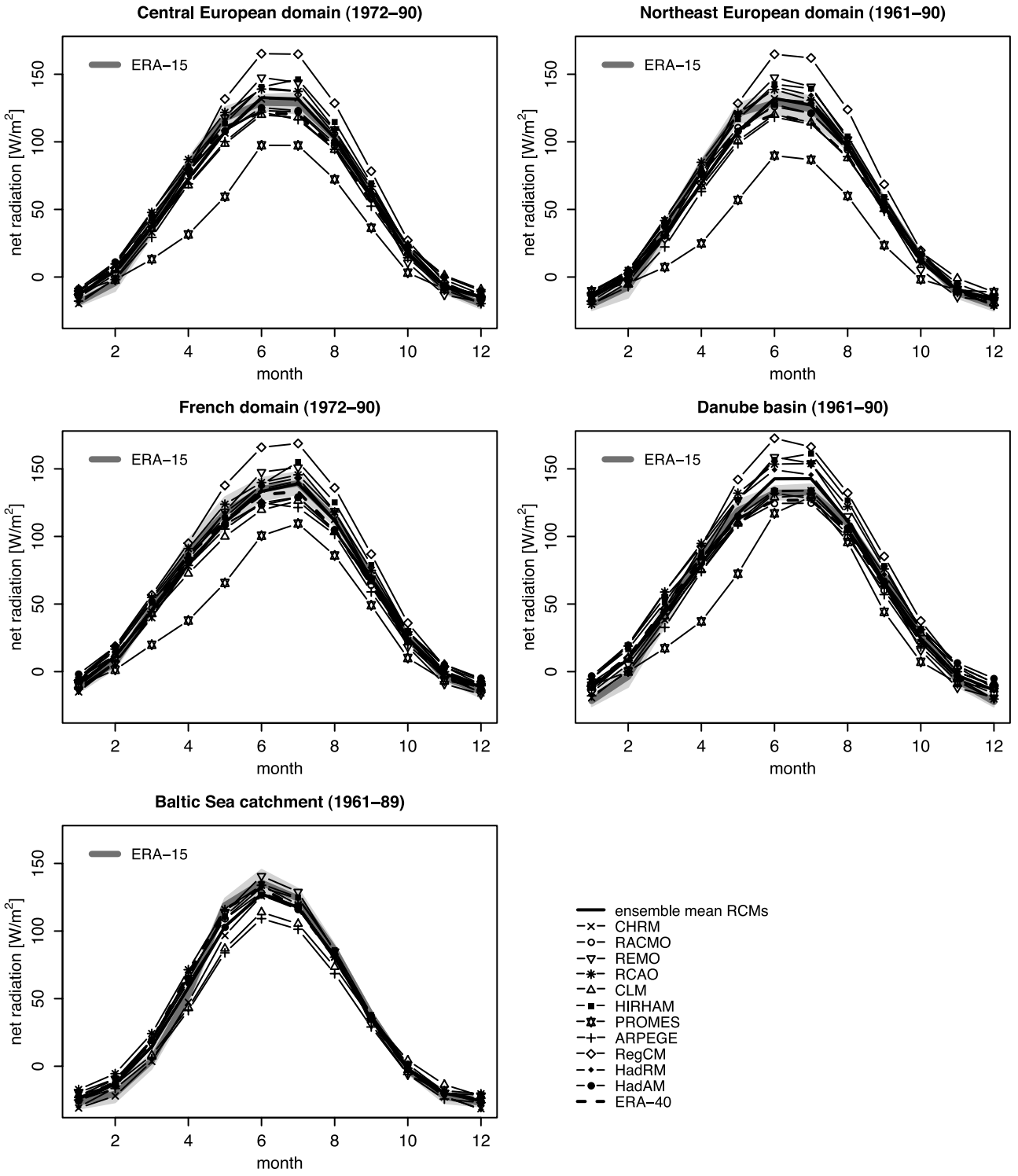

Figure 9. Same as Figure 2, but for net radiation (validation data is the ERA-15 reanalysis).

whereas the observed river runoff that also enters the BSWB diagnostics shows less interannual variability during summer (see Figure 8, e.g., Northeast European domain). The interannual variability of precipitation and runoff in the ensemble mean of the RCMs (not shown) agrees well with the observed variability. However, the year-to-year variability in simulated evapotranspiration is strongly underestimated. This is also the case for ERA-40 evapotranspiration, though the ERA-40 precipitation shows a realistic year-to-year variability (not shown).

[27] Overall, the simulated mean seasonal cycles of TWS variations (except in the Baltic region) as well as of evapotranspiration (in all domains) seem to be slightly shifted compared to the validation data and attain their minimum and maximum about one month too early. This is still the case when a one month delay in measured runoff

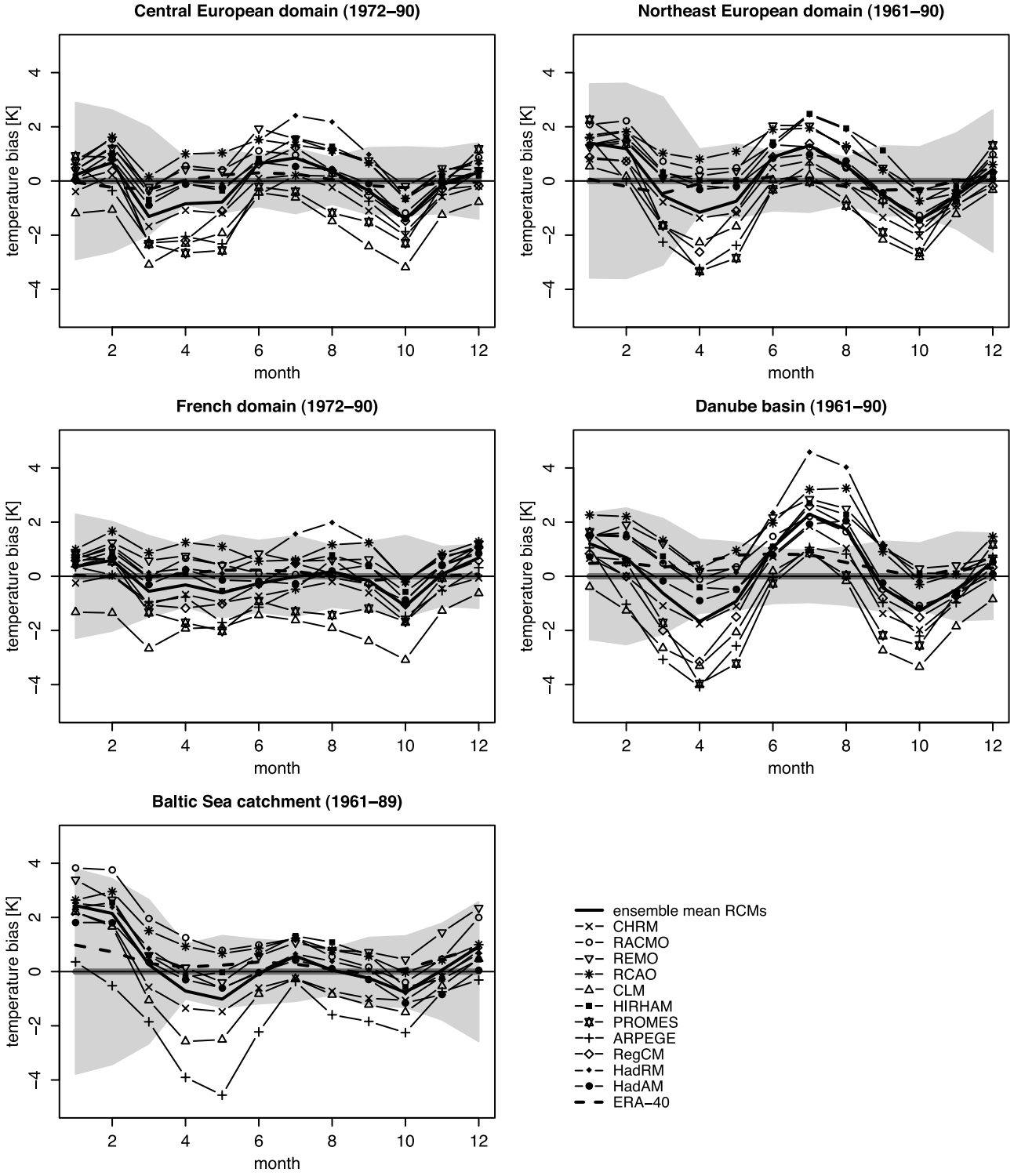

Figure 10. Same as Figure 2, but for the bias in modeled 2 m temperature (differences from observed CRU temperature data). The shaded area denotes ± one monthly standard deviation of the CRU data.

is taken into account for the diagnosis of the BSWB data (see section 2.5 and Figure 2, dashed grey lines).

[28] The simulated ERA-40 TWS variations show a pronounced underestimation in summer TWS decrease (except for the Baltic Sea catchment), and an overestimation in spring TWS reduction (not pronounced in the French domain; see Figure 2). In summer, this is likely related to the soil moisture increments added in the ERA-40 soil moisture analysis. This addition of water leads to a dampening of the decrease in summer TWS, as discussed in several previous studies [e.g., *Betts et al.*, 1998, 1999, 2003a; *Seneviratne et al.*, 2004; *Hirschi et al.*, 2006], and makes that the water balance of ERA-40 is not closed at the land surface [e.g., *Hagemann et al.*, 2005]. In spring, snow melt is immediately removed as runoff in ERA-40, whereas in reality it might refreeze deeper in the snowpack [*Betts et al.*, 2003b; *Hirschi et al.*, 2006]. This is visible in the overestimation of ERA-40 spring runoff (see Figure 8), and results in the overestimated TWS reduction in spring.

4. Seasonal Cycle of Hydrological Variables: Regional Analyses

4.1. Central and Northeast European Domains

[29] In the Central and Northeast European domains, most models overestimate the decrease in TWS during spring (mainly in April and May) and summer (mainly June and July, Figures 2 and 5). In spring and early summer seasons, these negative model biases in TWS variations appear related to a precedent overestimation of precipitation during winter and spring (Figure 6) and consequent overestimation of evapotranspiration (Figure 7). Note, though, that some of the precipitation and evapotranspiration biases may result from undercatch of solid precipitation by the rain gauges (since CRU precipitation is not corrected for gauge biases; see section 2.3). However, later in the summer, the negative biases in TWS variations in the Central European domain are associated with an underestimation of late summer precipitation, which also leads to underestimated late summer runoff.

[30] In autumn and winter, the increase in TWS is overestimated by the models, mainly as a consequence of too strong precipitation and underestimated early autumn evapotranspiration (as well as too low autumn runoff in the Central European domain). Consequently, the simulated mean annual TWS amplitudes are somewhat too large in the two domains (see Figure 5, Table 3, and the standard deviations σ of the modeled mean seasonal cycles of TWS variations in Figure 3).

4.2. French Domain and Danube Basin

[31] In the French domain (in June and July) and in the Danube basin (in July and August), the summer decrease in TWS is mostly underestimated by the models (Figure 2), i.e., the models show positive biases in summer TWS variations. In the Danube basin, this is associated with strongly underestimated summer evapotranspiration in most RCMs (Figure 7). This indicates water shortage in the models and suggests that they may reach water stress conditions too early in this region (also note that precipitation is continuously underestimated in the warm season; see Figure 6). Previous studies have often pointed to a "summer drying" issue of RCMs in southeastern Europe [e.g., *Hagemann et al.*, 2004]. This may be associated with a too low water-holding capacity of the model soils as the mean annual TWS amplitude appears underestimated (Figure 5 and Table 3). This is an important issue, in particular for climate change projections [*Seneviratne et al.*, 2006b]. In the French domain, the underestimation of summer TWS decrease is related to an overestimation of early summer precipitation.

[32] Overestimated precipitation in winter (in the French domain) and spring (in both domains) leads to overestimated spring evapotranspiration in most models, and thus to slightly negative spring biases in TWS variations. In autumn, the increase in TWS is overestimated in the Danube basin (mainly in September and October) as a consequence of too low evapotranspiration and runoff. In the French domain, the increase in model TWS is mainly overestimated in November and December, resulting from positive winter biases in precipitation. The resulting standard deviations σ of the modeled mean seasonal cycles of TWS variations are mostly too low in these domains (Figure 3).

4.3. Baltic Sea Catchment

[33] In the Baltic Sea catchment, the model ensemble mean of the seasonal cycles of TWS variations (Figures 2 and 3) and of absolute TWS (Figure 5) fit well the BSWB data. However, the spread between the models is large in winter and spring (over 1 mm/d in TWS variations). The excess of model precipitation in winter and spring (see Figure 6) is compensated by overestimated evapotranspiration and (in some models) runoff (Figures 7 and 8). Note that as mentioned in section 2.6, this domain is not covered by PROMES and RegCM.

5. Seasonal Cycle of Hydrological Variables: Individual Models

[34] Some model-specific characteristics can be observed in the various regions. Generally, the lower bound in TWS amplitude is defined by PROMES, showing a pronounced underestimation of the amplitude in all domains, i.e., less than half of the amplitude of the BSWB data (see Figure 5, Table 3, and standard deviations σ in Figure 3). This is related to strongly underestimated evapotranspiration mainly in spring and summer (Figure 7), and overestimated runoff in autumn and winter (Figure 8). The reduced evapotranspiration is on the one hand a consequence of a pronounced underestimation in net radiation (Figure 9). On the other hand, both the underestimation of evapotranspiration and the overestimation of runoff suggest an underestimation of the water-holding capacity or rooting depth used in this model.

[35] In the French, the Central and the Northeast European domains, the upper bound in TWS amplitude is set by RegCM and RACMO (Figures 3 and 5 and Table 3). The land surface schemes of both models (i.e., BATS1e and TESSEL respectively) have deep soils with 5 m extent (Table 2). These large storage capacities enable the absorption of the excess in winter and spring model precipitation (Figure 6), which is visible in the overestimation of water storage in winter in these domains (mainly from November to January, Figure 2). Driven by too high net radiation in

summer (Figure 9), the enhanced evapotranspiration in RegCM is maintained by the previously stored water (and also by too high summer precipitation) and results in a larger summer TWS decrease compared to most other models. In RACMO, the depletion of this water stored in the extensive soil is achieved through the positive summer runoff bias (in the Central European and the French domains). The effect of the larger soil depths can also be seen in the relatively high year-to-year variability in TWS variations of these models (Figure 4).

[36] The ARPEGE model exhibits a strongly overestimated cycle of TWS (Figures 2, 3, and 5) in the Baltic Sea catchment with an unrealistically high runoff peak in late spring (Figure 8). Spring runoff is also strongly overestimated in the other domains. This behavior seems to be associated with an excess snow accumulation in winter, leading to unrealistically high spring runoff [*Hagemann et al.*, 2004].

6. Interrelation of Biases and Processes

6.1. Bias Correlations

[37] The biases in the models' mean seasonal cycles in the various domains are analyzed here in more depth. Figures 11 and 12 display the mean monthly TWS biases (see Figure 5 and section 3.1) plotted against the mean monthly biases in simulated precipitation, evapotranspiration, runoff and temperature, respectively, for spring (MAM), summer (JJA) and autumn (SON). Each symbol refers to one month and one model. Significant correlations (on the $p = 0.05$ level) between the biases of the different models are denoted by an asterisk for the various domains.

[38] Figure 11 (top panels) shows that in spring, precipitation and evapotranspiration biases are in general positively correlated with simultaneous TWS biases (except in the Baltic Sea catchment). This points to a soil-driven spring evapotranspiration regime in the models. Spring temperature biases also show significantly positive correlations with the TWS biases in the French and Northeast European domains. However, temperature is mostly underestimated in the simulations. This may be linked to an average positive precipitation bias. In the Baltic Sea catchment, TWS biases are positively correlated with runoff biases, and negatively with temperature biases, showing the importance of TWS biases for these variables. Note that in this region, both precipitation and evapotranspiration are overestimated.

[39] In summer, in the Danube region, the well-know problem of exaggerated summer dryness can be see in the simulations with too low TWS, precipitation, and evapotranspiration. This may be due to a too strong soil moisture-precipitation coupling in the models. This is also the case for some models in other domains (e.g., for CLM in the Central and Northeast European domains). The summer dryness in the Danube basin also results in overestimated temperatures and underestimated runoff (Figure 12, middle panels). In the Baltic Sea catchment, summer TWS biases are significantly positively correlated with biases in precipitation and runoff. Thus, through TWS, positive (negative) biases in precipitation are transferred into positive (negative) runoff biases.

[40] In autumn, runoff biases are positively correlated with TWS biases in all domains, indicating a soil-controlled runoff regime in this season. In the Baltic Sea catchment, also precipitation, evapotranspiration and temperature biases display significantly positive correlations with the TWS biases, pointing to a soil-controlled evapotranspiration regime. On the other hand, biases in evapotranspiration are significantly negatively correlated with TWS biases in the French domain, indicating an atmospheric-controlled evapotranspiration regime. In the Danube basin finally, autumn temperature biases show a significantly negative correlation with TWS biases, indicating a soil-driven temperature regime, in which too high (low) temperatures are related to an underestimation (overestimation) of TWS.

[41] Overall, this analysis shows some strong correlations between TWS biases and biases in other climatic variables in all three seasons. This demonstrates the importance of validating TWS in climate simulations, though the exact causal links between the biases cannot be inferred through correlations analysis alone.

6.2. Lagged Correlations

[42] Here we analyze the interannual variability of the model and validation data by investigating the lagged correlations between different variables (i.e., spring to summer and summer to autumn correlations), focusing on the effects of absolute TWS on other simulated quantities (see Figures 13 and 14; dotted horizontal lines depict the $p = 0.05$ and $p = 0.01$ significance levels). The same validation data sets as in Figures 2–8 and 10 are applied. Each panel also includes the respective ERA-40 correlations for comparison. Since only the climatological runoff was available for HadAM (not the full time series), no correlations involving this parameter can be calculated for this model.

[43] Most models and the diagnostic BSWB data exhibit a significant positive relation between spring and summer TWS, representing the memory effect of TWS in the climate system (Figure 13, top left panel). In the Central European and the French domains, this effect is even larger in the BSWB data than in the models. Likely as a result of its limited storage capacity (see section 5), PROMES shows smaller or even negative correlations and thus a reduced memory effect. The same is also demonstrated by the small or even negative response of summer (autumn) evapotranspiration on spring (summer) TWS, while most other models and the validation data show positive correlations (Figures 13 and 14, middle left panels). Anomalies in TWS seem to be directed instantly to runoff by PROMES, which is demonstrated by the strong positive correlations of TWS with simultaneous runoff in both spring and summer (not shown). This corresponds with earlier findings showing a strong runoff response of PROMES to anomalies in atmospheric moisture convergence [*van den Hurk et al.*, 2005]. On the other hand, models with larger storage capacity (i.e., RACMO and RegCM) show relatively large correlations between spring and summer TWS in most regions, indicating a larger memory effect. The small spring to summer TWS memory of ARPEGE in the Northeast European domain and the Danube basin is likely related to its large positive biases in spring runoff, which removes positive spring anomalies in TWS (see section 5 and Figure 8). These results confirm that soil moisture memory

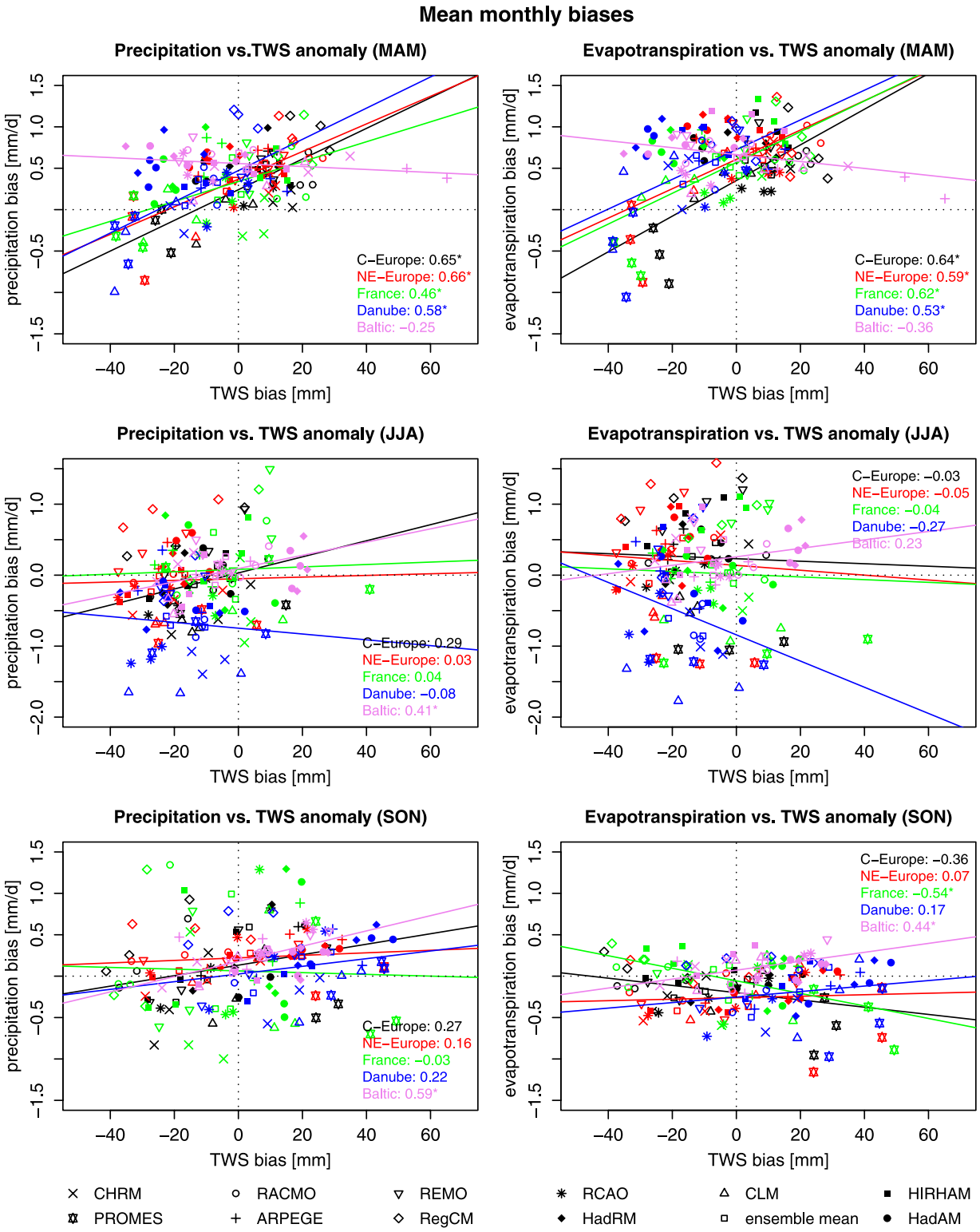

Figure 11. Mean monthly model biases in precipitation and evapotranspiration versus mean monthly TWS biases (validation data as in Figures 5–7): for spring (MAM, top), summer (JJA, middle) and autumn (SON, bottom), in the Central European (black), Northeast European (red), and French (green) domains, the Danube basin (blue), and the Baltic Sea catchment (violet). Also displayed are the respective regression lines and correlation coefficients for the 10 regional simulations (asterisk (*), significant on $p = 0.05$ level).

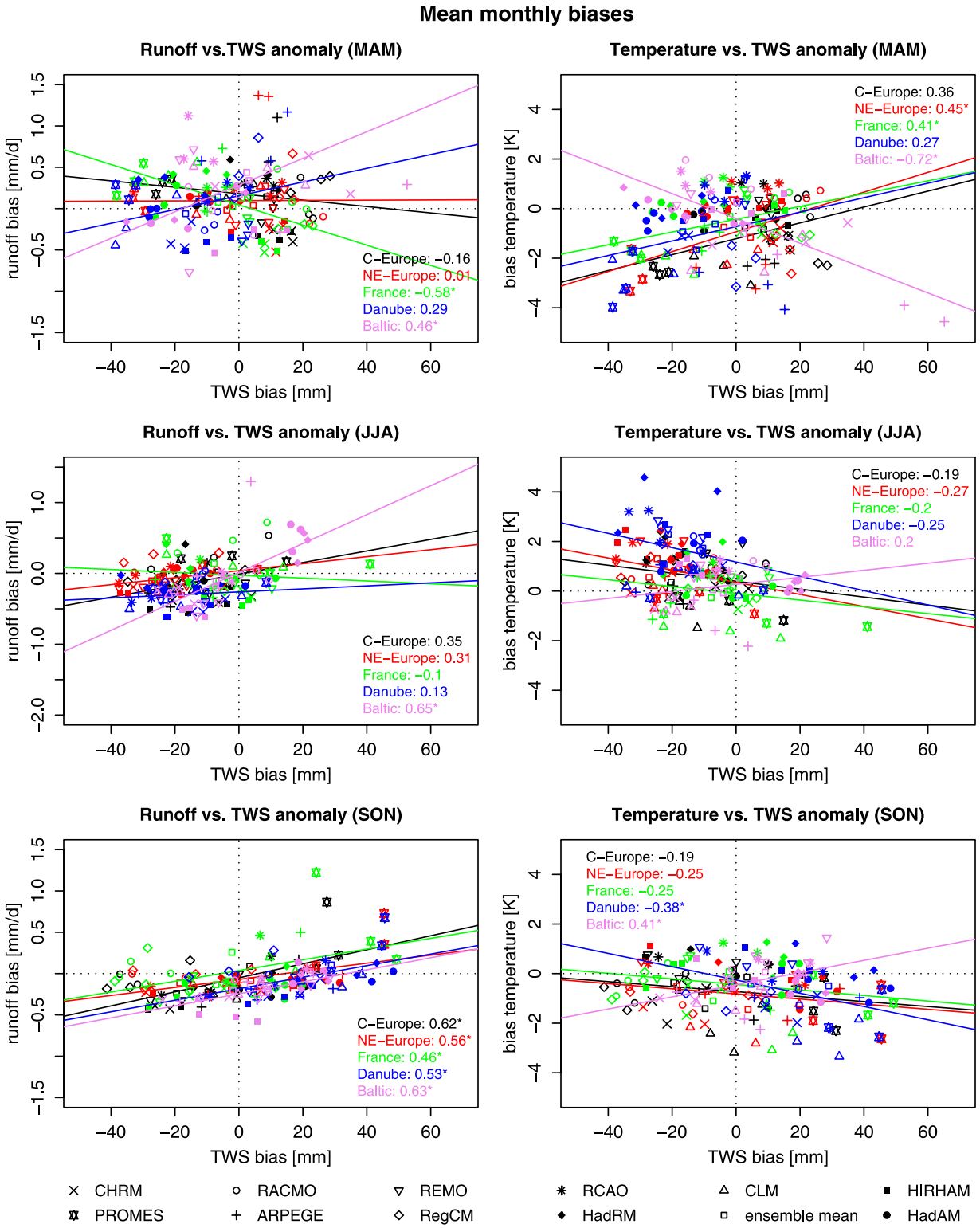

Figure 12. Same as Figure 11, but for mean monthly biases in runoff and temperature versus mean monthly TWS biases (validation data as in Figures 5, 8, and 10).

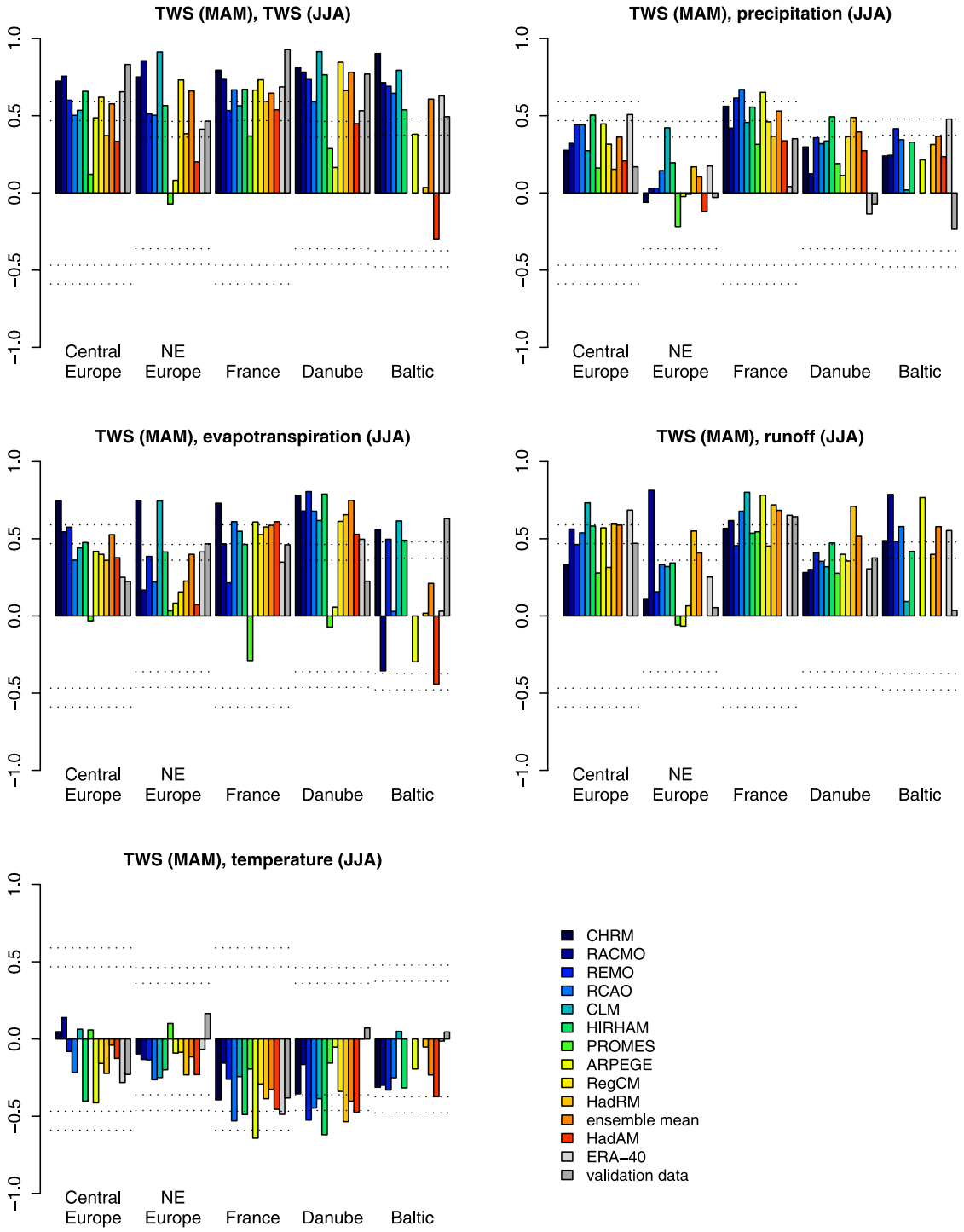

Figure 13. Correlations between absolute spring TWS and summer values of other variables (same data as in Figures 2–8 and 10). Also shown in each panel are the respective correlations of ERA-40. The dotted horizontal lines depict the $p = 0.05$ and $p = 0.01$ significance levels.

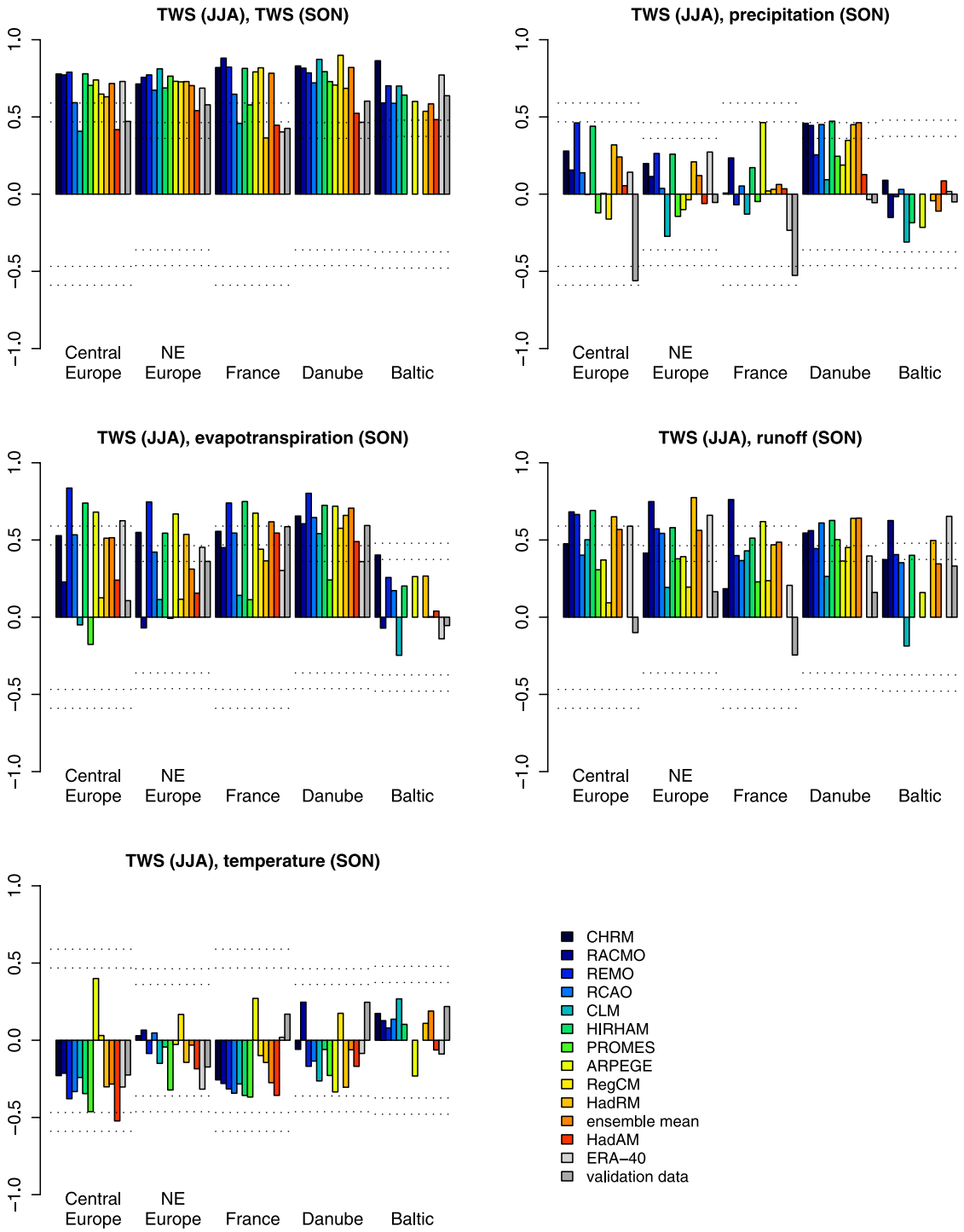

Figure 14. Same as Figure 13, but for summer to autumn values.

in models is generally controlled by water holding capacity on the one hand and by the sensitivity of evapotranspiration and runoff to soil moisture content at the lower and upper bounds of the soil moisture range on the other hand [e.g., *Delworth and Manabe*, 1988; *Koster and Suarez*, 2001; *Seneviratne et al.*, 2006a]. Between summer and autumn, the simulated memory in TWS (Figure 14, top left panel) is mostly overestimated compared to the diagnostic BSWB data, possibly due to an underestimation of precipitation in fall in the models (Figure 6).

[44] For most models and regions, the memory effect of TWS results in positive correlations between spring TWS and summer evapotranspiration and runoff (however not always significant, Figure 13). The validation data shows a similar signal, but that is only significant for evapotranspiration in the Northeast European domain and the Baltic region as well as for runoff in the French domain and the

Danube basin. The correlations with spring TWS are less pronounced for modeled summer precipitation, but a significant positive soil moisture-precipitation feedback can be observed for some models (mainly in the French domain and in the Danube basin). Nowhere in the validation data this positive feedback is significant. On the other hand, simulated spring TWS is negatively correlated with summer temperature (however only significant for models in the French domain and in the Danube basin). As for precipitation, observed summer temperature nowhere shows significant anticorrelations with spring TWS. Thus these feedbacks may be overestimated in the models. Note that in the Danube basin, already the driving model HadAM shows a significant anticorrelation between spring TWS and summer temperature.

[45] In most models and regions, also autumn evapotranspiration (in the Baltic Sea catchment only for CHRM) and runoff are significantly correlated with summer TWS. In the validation data, these correlations are only significant for evapotranspiration in the French and the Danube regions.

[46] For autumn precipitation, two striking features can be identified. First, there is a positive relation between summer TWS and autumn precipitation in the models for the Danube basin, which is absent in the other domains. Note, however, that the observations in the Danube basin suggest that this positive correlation might be erroneous.

[47] Moreover, the validation data surprisingly show significantly negative correlations between summer TWS and observed autumn precipitation in the Central European and French domains, which are absent in the models (Figure 14, top right panel). Also spring TWS, as well as spring precipitation are both significantly anticorrelated with autumn precipitation in the validation data (not shown). These spring to autumn anticorrelations are also apparent in RCM simulations with the CHRM model driven by ERA-40 boundary conditions (not shown). The origin of these correlations is likely due to atmospheric variability not captured by the driving HadAM. However, the exact reasons for this peculiar summer-autumn link will be the subject of future investigations.

7. Climate-Change Signal

[48] This paper mainly focuses on the control period of the simulations, thus no extensive analysis is provided for the scenario runs (for this, see the PRUDENCE special issue of Climatic Change [*Christensen et al.*, 2007]). Nevertheless, some comments concerning the simulated changes of the TWS cycles are given below. A more in-depth analysis of projected TWS (mainly of soil moisture) and its links to future summer variability in precipitation and temperature is given by *Vidale et al.* [2007].

[49] The response of the modeled seasonal cycle of monthly TWS variations to the A2 scenario (i.e., scenario minus control run) is displayed in Figure 15 for the various domains. The seasonal TWS cycle is generally enhanced in all regions, with a stronger decrease (increase) in storage during summer (winter), and lower absolute soil water values during summer. The overall absolute change in TWS amplitude is largest in the French domain. Having a much deeper soil and larger water reservoirs than most other PRUDENCE models (see Table 2), RACMO shows a comparable large increase in the amplitude of the seasonal TWS cycle (e.g., in the Central European and French domains). In contrast to most other models, ARPEGE shows a decreased winter TWS accumulation, likely due to a reduction of the presently overestimated snow accumulation (see section 5) in a warmer climate.

[50] The projected enhancement of the seasonal TWS cycle corresponds with findings from other PRUDENCE studies showing an increase in winter precipitation, and a decrease in summer precipitation in most of Europe [*Räisänen et al.*, 2004; *Christensen and Christensen*, 2007], which is accompanied by an increase in summer temperature variability [*Schär et al.*, 2004b; *Vidale et al.*, 2007; *Lenderink et al.*, 2007; *Seneviratne et al.*, 2006b] and precipitation variability [*Vidale et al.*, 2007] as well as an increased incidence of heavy summer precipitation events [*Christensen and Christensen*, 2003; *Frei et al.*, 2006]. The increase in summer temperature variability is visible in Figure 16, showing the projected mean relative changes (i.e., (*scen-ctrl*)/*ctrl*) of the interannual summer variability in temperature and TWS variations. The future year-to-year variability in monthly summer TWS variations is reduced in the Central European domain in several models, while temperature and precipitation (not shown) variability is enhanced at the same time. Mainly in August, the year-to-year variability in TWS variations drops below present-day values in many models (not shown). This reduction in variability is likely related to more frequently exhausted model soil water reservoirs by the end of summer, leading to a shutdown of evapotranspiration [see also *Vidale et al.*, 2007]. A decrease in projected TWS variability is also visible in the French domain and in the Danube basin, where it is however also related to a simultaneous reduction in precipitation variability in several models (not shown).

[51] Comparing the lagged correlations from the control period (see section 6.2) with the ones from the scenario period reveals a stronger relation between spring TWS and summer temperature in the future (Figure 17, top). While in the control period, only models in the French domain and in the Danube basin show significant negative correlations between these two variables, the future simulations display this effect for most models in all regions except in the Baltic Sea catchment. The same is to a lesser extent also true for the correlations between summer TWS and autumn temperature (Figure 17, bottom). This corresponds with recent findings showing a future shift in the climate regimes within Europe, with Central and Eastern Europe becoming susceptible to the effects of land-atmosphere coupling, with consequent impacts on summer temperature variability [*Seneviratne et al.*, 2006b].

8. Conclusions

[52] The seasonal evolution of TWS in an ensemble of regional climate simulations driven by the same boundary conditions has been analyzed in five large European domains, using a recently published basin-scale data set of diagnosed monthly TWS variations (BSWB data set [*Hirschi et al.*, 2006; *Seneviratne et al.*, 2004]) as well as other validation data sets (e.g., observed precipitation, runoff and temperature as well as diagnosed evapotranspiration). It is important to note that the RCMs are driven by a free-running

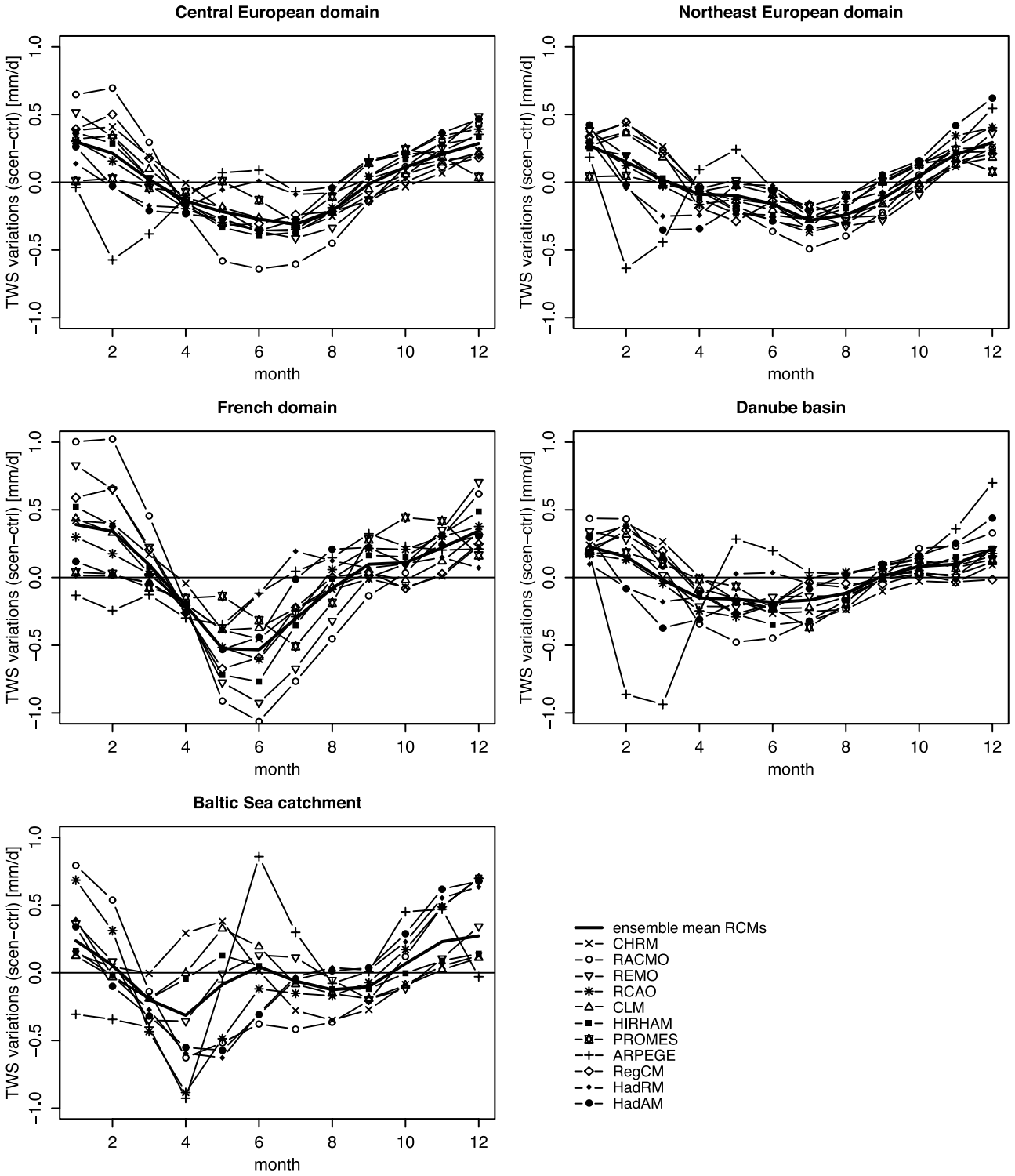

Figure 15. Changes in monthly TWS variations (scenario-control) in the European domains: the 10 regional climate simulations and their ensemble mean as well as the global driving model (HadAM) are shown.

atmospheric GCM with observed sea-surface forcing. Thus large-scale circulation biases will affect the results, and discrepancies between model and observations are not exclusively related to RCM-internal biases (e.g., to land-surface processes or other parameterizations). Nevertheless, our validation provides a detailed analysis of the water cycle in current state-of-the-art climate models and scenarios.

[53] The differences between individual models in the mean seasonal cycle of TWS variations are sometimes considerable and can amount to more than 1 mm/d in summer and winter. However, most simulated climatologies

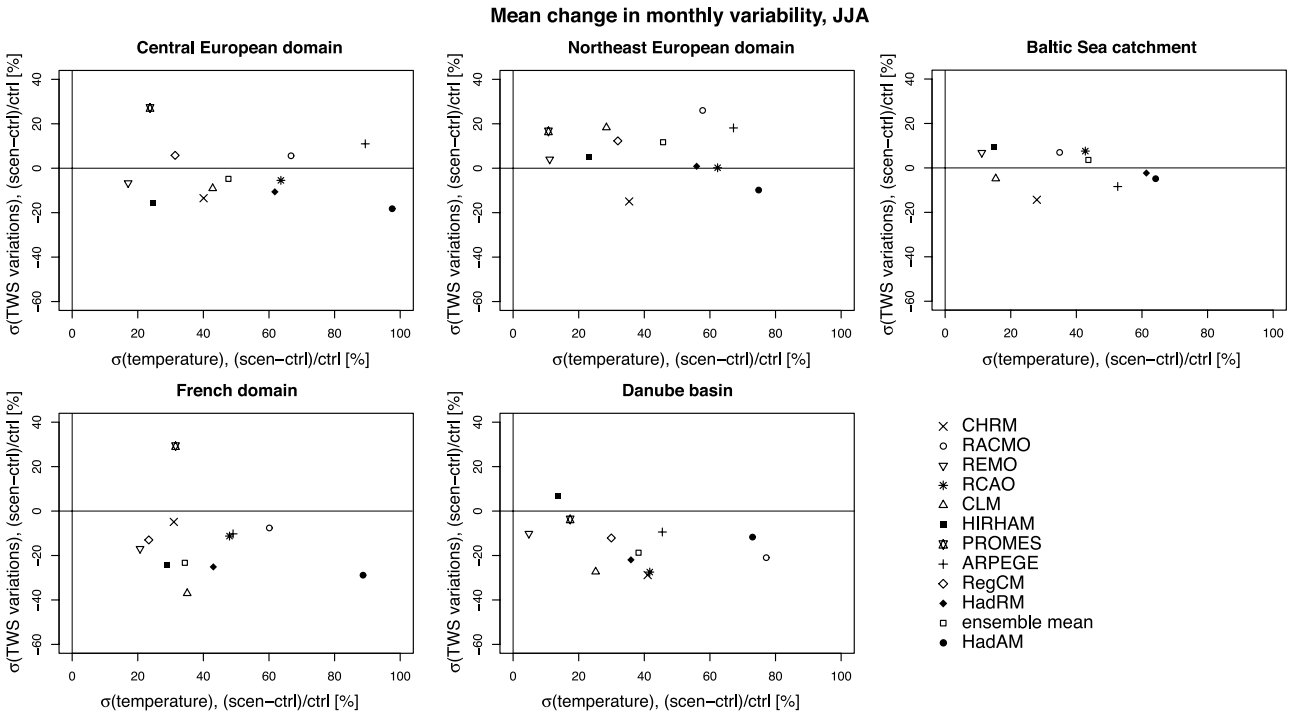

Figure 16. Mean relative changes (i.e., (*scen-ctrl*)/*ctrl*) of the interannual summer variability: temperature versus monthly TWS variations. The 10 regional climate simulations and their ensemble mean as well as the global driving model (HadAM) are shown.

lie within ± one monthly standard deviation of the diagnostic BSWB data. The phase of the modeled mean seasonal cycles of TWS variations appears to be slightly shifted compared to the BSWB estimates with the peak in TWS reduction occurring about one month too early in the models. This is still the case when a time delay of one month in observed downstream station runoff is accounted for in the BSWB estimates (Figure 2, dashed grey line). Likewise, when the regional simulations are compared with the diagnosed evapotranspiration, a similar phase shift is apparent. However, note that since the diagnosed TWS variations and evapotranspiration are based on the same ERA-40 data, these validation data sets are not strictly independent. Whether the phase of the regional simulations or of ERA-40 is correct cannot be said conclusively, although the latter is constrained by radiosonde observations. Generally, the deviations of the individual models from the diagnostic validation data of monthly TWS

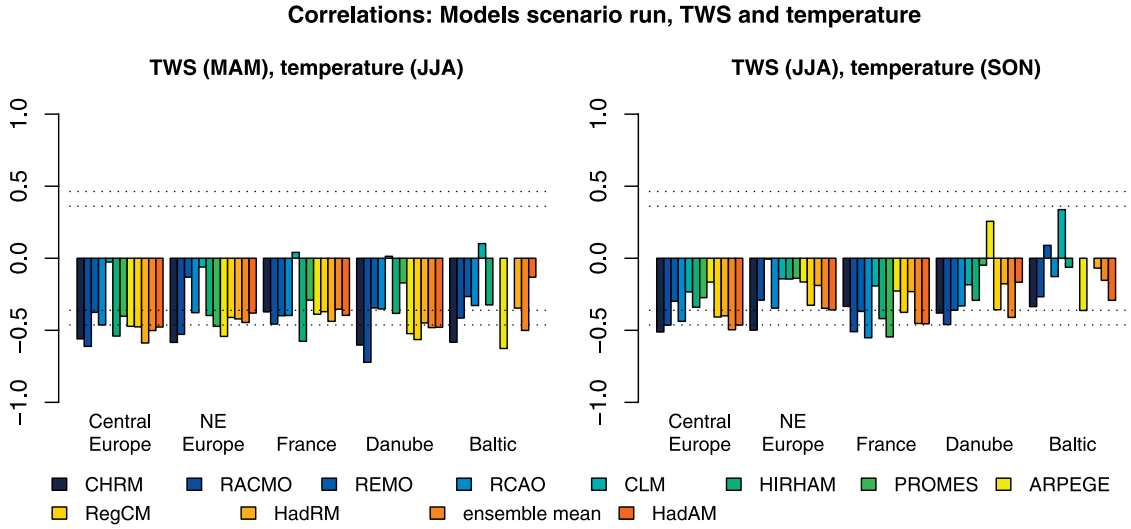

Figure 17. Correlations (left) between absolute spring TWS and summer temperature as well as (right) between summer TWS and autumn temperature for the simulated scenario period 2071–2100. The dotted horizontal lines depict the $p = 0.05$ and $p = 0.01$ significance levels.

variations can be explained as a result of biases in the simulated hydrological fluxes (i.e., precipitation, runoff, evapotranspiration).

[54] Compared to the BSWB data, most regional simulations overestimate the mean annual TWS amplitudes in the Central and Northeast European domains, and underestimate it in the Danube basin (see Table 3 and Figure 5). In the French domain and in the Baltic Sea catchment, the models are closer to the BSWB data in terms of annual TWS amplitudes.

[55] Common to all regions are the positive model biases in precipitation in winter (except for the Danube basin) and spring, likely resulting from the positive winter bias in the strength of westerly winds in the driving model HadAM [*van Ulden et al.*, 2007]. Part of the apparent model biases may result from undercatch of solid precipitation by the rain gauges. The excess of precipitation leads to overestimated winter and spring evapotranspiration and to slightly enhanced winter or spring runoff as well as to increased spring TWS reduction (except for the Baltic Sea catchment). In the Central and Northeast European domains, this has also consequences on summer evapotranspiration (i.e., too high June and July evapotranspiration in most models), and leads then to overestimated summer TWS decrease. On the other hand, in the French domain and in the Danube basin, the reduction in summer TWS is mostly underestimated by the models, mainly as a consequence of too low summer evapotranspiration and runoff in the Danube region, and of overestimated early summer precipitation in the French domain. In the Danube basin, the too low reduction of summer TWS is associated with underestimated summer precipitation due to water shortage in the models (i.e., the mean monthly biases in TWS variations are negatively correlated with mean monthly precipitation biases, not shown), and consequently limited evapotranspiration (while summer net radiation is mostly overestimated). This corresponds to the previously observed summer drying problem in southeastern Europe [*Hagemann et al.*, 2004]. Some models behave similarly also in other domains, i.e., displaying too low summer precipitation and evapotranspiration at the same time, and thus an underestimation in TWS reduction due to water stress (e.g., CLM and HadRM in the French domain). These models with strong summer drying tend to enhance or maintain the positive summer bias in easterly winds (i.e., leading to too warm and dry conditions) imported from the global driving model HadAM, while models with less summer drying (e.g., RegCM and RACMO) seem to be rather insensitive to this easterly bias [*Lenderink et al.*, 2007; *van Ulden et al.*, 2007].

[56] Compared with validation data, the regional simulations often show stronger time-lagged correlations between TWS and other variables (see section 6.2), e.g., for the correlations between spring TWS and summer precipitation and evapotranspiration. Moreover, the strengths of the relations differ considerably between individual models in some cases (e.g., see the correlations between spring TWS and summer evapotranspiration) and are dependent on individual models characteristics (e.g., on the model soil depth and its storage capacity [see also *van den Hurk et al.*, 2005]). In general, the seasonal evolution of TWS depends on numerous parameterizations (e.g., atmospheric radiation, cloud-radiation interactions, runoff formation, and transpiration; see also Tables 1 and 2), and it is not feasible here to ascribe a particular model failure to one particular parameterization scheme. Nevertheless, these model uncertainties influence the quality of future climate projections. The use of the multimodel ensemble mean may help in this context to reduce the uncertainty, which is included in a single model. Overall, the A2 scenario runs suggest that the seasonal cycle of TWS will be enlarged in the future, with lower soil water values during summer [see also *Vidale et al.*, 2007]. This corresponds with findings of recent studies, which show an increased risk of future summer dryness in southern and central Europe [e.g., *Wetherald and Manabe*, 2002; *Manabe et al.*, 2004; *Räisänen et al.*, 2004; *Schär et al.*, 2004b; *Seneviratne et al.*, 2006b].

[57] **Acknowledgments.** We would like to thank the PRUDENCE community and David Hein (Met Office, UK) for providing the model data, the team of the Global Runoff Data Centre (Koblenz, Germany; Thomas Lüllwitz), and the local providers of runoff data. Sincere thanks to Erich Fischer for providing data of the ERA-40 CHRM run and for many useful comments and discussions as well as Reinhard Schiemann for providing the R-code for Figure 3. Comments from three anonymous reviewers are also gratefully acknowledged. This research was supported by the Swiss National Science Foundation (NCCR Climate) and by the 5th (PRUDENCE) and 6th (ENSEMBLES and CECILIA) Framework Programmes of the European Union.

References

Allen, M. R., and W. J. Ingram (2002), Constraints on future changes in climate and the hydrologic cycle, *Nature*, *419*(6903), 224–232.

Bergström, S., and B. Carlsson (1993), Hydrology of the Baltic basin — Inflow of fresh water from rivers and land for the period 1950–1990, *SMHI Rep. RH 7*, Swed. Meteorol. and Hydrol. Inst., Norrköping, Sweden.

Betts, A. K. (2004), Understanding hydrometeorology using global models, *Bull. Am. Meteorol. Soc.*, *85*(11), 1673–1688.

Betts, A. K., P. Viterbo, and E. Wood (1998), Surface energy and water balance for the Arkansas-Red river basin from the ECMWF reanalysis, *J. Clim.*, *11*, 2881–2897.

Betts, A. K., J. H. Ball, and P. Viterbo (1999), Basin-scale surface water and energy budgets for the Mississippi from the ECMWF reanalysis, *J. Geophys. Res.*, *104*(D16), 19,293–19,306.

Betts, A. K., J. H. Ball, M. Bosilovich, P. Viterbo, Y. Zhang, and W. B. Rossow (2003a), Intercomparison of water and energy budgets for five Mississippi subbasins between ECMWF reanalysis (ERA-40) and NASA Data Assimilation Office fvGCM for 1990–1999, *J. Geophys. Res.*, *108*(D16), 8618, doi:10.1029/2002JD003127.

Betts, A. K., J. H. Ball, and P. Viterbo (2003b), Evaluation of the ERA-40 surface water budget and surface temperature for the Mackenzie River basin, *J. Hydrometeorol.*, *4*, 1194–1211.

Bringfelt, B., J. Räisänen, S. Gollvik, G. Lindström, L. P. Graham, and A. Ullerstig (2001), The land surface treatment for the Rossby Centre Regional Atmospheric Climate Model version 2 (RCA2), *Rep. Meteorol. Climatol. 98*, Swed. Meteorol. and Hydrol. Inst., Norrköping, Sweden.

Christensen, J. H., and O. B. Christensen (2003), Climate modelling: Severe summertime flooding in Europe, *Nature*, *421*, 805–806.

Christensen, J. H., and O. B. Christensen (2007), A summary of the PRUDENCE model projections of changes in European climate by the end of this century, *Clim. Change*, *81*, suppl. 1, 7–30.

Christensen, J. H., O. B. Christensen, P. Lopez, E. van Meijgaard, and M. Botzet (1996), The HIRHAM4 regional atmospheric climate model, *Sci. Rep. 96-4*, 51 pp., Dan. Meteorol. Inst., Copenhagen.

Christensen, J. H., T. R. Carter, M. Rummukainen, and G. Amanatidis (2007), Evaluating the performance and utility of regional climate models: The PRUDENCE project, *Clim. Change*, *81*, suppl. 1, 1–6.

Cox, P. M., R. A. Betts, C. B. Bunton, R. L. H. Essery, P. R. Rowntree, and J. Smith (1999), The impact of new land surface physics on the GCM simulation of climate and climate sensitivity, *Clim. Dyn.*, *15*, 183–203.

Delworth, T. L., and S. Manabe (1988), The influence of potential evaporation on the variabilities of simulated soil wetness and climate, *J. Clim.*, *1*(5), 523–547.

Déqué, M., P. Marquet, and R. G. Jones (1998), Simulation of climate change over Europe using a global variable resolution general circulation model, *Clim. Dyn.*, *14*(3), 173–189.

Dickinson, R. E. (1984), Modeling evapo-transpiration for the three-dimensional global climate models, in *Climate Processes and Climate Sensitivity*, *Geophys. Monogr. Ser.*, vol. 29, edited by J. E. Hansons and T. Takahashi, pp. 58–72, AGU, Washington, D. C.

Dickinson, R. E., A. Henderson-Sellers, and P. J. Kennedy (1993), Biosphere-Atmosphere Transfer Scheme (BATS) Version 1e as coupled to the NCAR Community Climate Model, *NCAR Tech. Note NCAR/TN-387*, Natl. Cent. for Atmos. Res., Boulder, Colo.

Döscher, R., U. Willen, C. Jones, A. Rutgersson, H. E. M. Meier, U. Hansson, and L. P. Graham (2002), The development of the coupled regional ocean-atmosphere model RCAO, *Boreal Environ. Res.*, *7*, 183–192.

Douville, H., S. Planton, J.-F. Royer, D. B. Stephenson, S. Tyteca, L. Kergoat, S. Lafont, and R. A. Betts (2000), The importance of vegetation feedbacks in doubled-CO_2 climate experiments, *J. Geophys. Res.*, *105*(D11), 14,841–14,861.

Ducoudré, N. I., K. Laval, and A. Perrier (1993), SECHIBA, a new set of parameterizations of the hydrologic exchanges at the land-atmosphere interface within the LMD atmospheric general circulation model, *J. Clim.*, *6*(2), 248–273.

Eltahir, E. A. B. (1998), A soil moisture-rainfall feedback mechanism. 1. Theory and observations., *Water Resour. Res.*, *34*(4), 765–776.

Fischer, E. M., S. I. Seneviratne, P. L. Vidale, D. Lüthi, and C. Schär (2007), Soil moisture-atmosphere interactions during the 20 03 European summer heatwave, *J. Clim.*, *20*(20), 5081–5099.

Frei, C., R. Schll, S. Fukutome, J. Schmidli, and P. L. Vidale (2006), Future change of precipitation extremes in Europe: Intercomparison of scenarios from regional climate models, *J. Geophys. Res.*, *111*, D06105, doi:10.1029/2005JD005965.

Gilgen, H., and A. Ohmura (1999), The Global Energy Balance Archive (GEBA), *Bull. Am. Meteorol. Soc.*, *80*, 831–850.

Giorgi, F., M. R. Marinucci, and G. T. Bates (1993a), Development of a second generation regional climate model (RegCM2). Part I: Boundary layer and radiative transfer processes, *Mon. Weather Rev.*, *121*(10), 2794–2813.

Giorgi, F., M. R. Marinucci, G. T. Bates, and G. D. Canio (1993b), Development of a second generation regional climate model (RegCM2). Part II: Convective processes and assimilation of lateral boundary conditions, *Mon. Weather Rev.*, *121*(10), 2814–2832.

Haddeland, I., T. Skaugen, and D. P. Lettenmaier (2006), Anthropogenic impacts on continental surface water fluxes, *Geophys. Res. Lett.*, *33*, L08406, doi:10.1029/2006GL026047.

Hagemann, S., and L. Dümenil (2001), Validation of the hydrological cycle of ECMWF and NCEP reanalyses using the MPI hydrological discharge model, *J. Geophys. Res.*, *106*, 1503–1510.

Hagemann, S., and L. Dümenil (2003), Improving a subgrid runoff parameterization scheme for climate models by the use of high resolution data derived from satellite observations, *Clim. Dyn.*, *21*, 349–359.

Hagemann, S., and D. Jacob (2007), Gradient in the climate change signal of European discharge predicted by a multi-model ensemble, *Clim. Change*, *81*, suppl. 1, 309–327.

Hagemann, S., B. Machenhauer, R. Jones, O. B. Christensen, M. Déqué, D. Jacob, and P. L. Vidale (2004), Evaluation of water and energy budgets in regional climate models applied over Europe, *Clim. Dyn.*, *23*(5), 547–567.

Hagemann, S., K. Arpe, and L. Bengtsson (2005), Validation of the hydrological cycle of ERA-40, *ERA-40 Proj. Rep. Ser. 24*, Eur. Cent. for Medium-Range Wather Forecasts, Reading, U. K.

Hanasaki, N., S. Kanae, and T. Oki (2006), A reservoir operation scheme for global river routing models, *J. Hydrol.*, *327*(1–2), 22–41.

Hirschi, M., S. I. Seneviratne, and C. Schär (2006), Seasonal variations in terrestrial water storage for major midlatitude river basins, *J. Hydrometeorol.*, *7*(1), 39–60.

Jacob, D. (2001), A note to the simulation of the annual and inter-annual variability of the water budget over the Baltic Sea drainage basin, *Meteorol. Atmos. Phys.*, *77*, 61–73.

Jacob, D., et al. (2007), An inter-comparison of regional climate models for Europe: Model performance in present-day climate, *Clim. Change*, *81*, suppl. 1, 31–52.

Jacobsen, I., and E. Heise (1982), A new economic method for the computation of the surface temperature in numerical models, *Contrib. Atmos. Phys.*, *55*, 128–141.

Jones, R., J. Murphy, D. Hassell, and R. Taylor (2001), Ensemble mean changes in a simulation of the European climate of 2071–2100, using the new Hadley Centre regional climate modelling system HadAM3H/HadRM3H, report, Hadley Centre, Met Off., London.

Kleinn, J., C. Frei, J. Gurtz, D. Lthi, P. L. Vidale, and C. Schr (2005), Hydrologic simulations in the Rhine basin driven by a regional climate model, *J. Geophys. Res.*, *110*, D04102, doi:10.1029/2004JD005143.

Koster, R. D., and M. J. Suarez (2001), Soil moisture memory in climate models, *J. Hydrometeorol.*, *21*, 558–570.

Koster, R. D., et al. (2004), Regions of strong coupling between soil moisture and precipitation, *Science*, *305*(5687), 1138–1140.

Koster, R. D., et al. (2006), GLACE: The Global Land-Atmosphere Coupling Experiment. Part I: Overview, *J. Hydrometeorol*, *7*(4), 590–610.

Legates, D. R., and C. J. Willmott (1990), Mean seasonal and spatial variability in gauge-corrected, global precipitation, *Int. J. Climatol.*, *10*, 111–127.

Lenderink, G., B. van den Hurk, E. van Meijgaard, A. van Ulden, and H. Cuijpers (2003), Simulation of present-day climate in RACMO2: First results and model developments, *TR 252*, 24 pp., R. Neth. Meteorol. Inst., Amsterdam.

Lenderink, G., A. van Ulden, B. van den Hurk, and E. van Meijgaard (2007), Summertime inter-annual temperature variability in an ensemble of regional model simulations: Analysis of the surface energy budget, *Clim. Change*, *81*, suppl. 1, 233–247.

Manabe, S. (1969), Climate and ocean circulation. 1. The atmospheric circulation and the hydrology of the Earth's surface, *Mon. Weather Rev.*, *97*(11), 739–774.

Manabe, S., R. T. Wetherald, P. C.D. Milly, T. L. Delworth, and R. J. Stouffer (2004), Century-scale change in water availability: CO_2-quadrupling experiment, *Clim. Change*, *64*, 59–76.

Manzi, A. O., and S. Planton (1994), Implementation of the ISBA parameterization scheme for land surface processes in a GCM—An annual cycle experiment, *J. Hydrol.*, *155*(3–4), 353–387.

Milly, P. C. D., R. T. Wetherald, K. A. Dunne, and T. L. Delworth (2002), Increasing risks of great floods in a changing climate, *Nature*, *415*, 514–517.

Milly, P. C. D., K. A. Dunne, and A. V. Vecchia (2005), Global pattern of trends in streamflow and water availability in a changing climate, *Nature*, *438*, 347–350.

New, M., M. Hulme, and P. Jones (1999), Representing twentieth-century space-time climate variability. part i: Development of a 1961–90 mean monthly terrestrial climatology, *J. Clim.*, *12*(3), 829–856.

New, M., M. Hulme, and P. Jones (2000), Representing twentieth-century space-time climate variability. part ii: Development of 1901–96 monthly grids of terrestrial surface climate, *J. Clim.*, *13*(13), 2217–2238.

Pitman, A. J. (2003), The evolution of, and revolution in, land surface schemes designed for climate models, *Int. J. Climatol.*, *23*, 479–510, doi:10.1002/joc.893.

Pope, D. V., M. Gallani, R. Rowntree, and A. Stratton (2000), The impact of new physical parameterizations in the Hadley Centre climate model: HadAM3, *Clim. Dyn.*, *16*(2–3), 123–146.

Räisänen, J., U. Hansson, A. Ullerstig, R. Döscher, L. P. Graham, C. Jones, H. E. M. Meier, P. Samuelsson, and U. Willen (2004), European climate in the late twenty-first century: Regional simulations with two driving global models and two forcing scenarios, *Clim. Dyn.*, *22*, 13–31.

Rasmusson, E. M. (1968), Atmospheric water vapor transport and the water balance of North America. II. Large-scale water balance investigations, *Mon. Weather Rev.*, *96*(10), 720–734.

Rayner, N. A., D. E. Parker, E. B. Horton, C. K. Folland, L. V. Alexander, D. P. Rowell, E. C. Kent, and A. Kaplan (2003), Global analyses of sea surface temperature, sea ice, and night marine air temperature since the late nineteenth century, *J. Geophys. Res.*, *108*(D14), 4407, doi:10.1029/2002JD002670.

Robock, A., K. Y. Vinnikov, G. Srinivasan, J. K. Entin, S. E. Hollinger, N. A. Speranskaya, S. Liu, and A. Namkhai (2000), The Global Soil Moisture Data Bank, *Bull. Am. Meteorol. Soc.*, *81*(6), 1281–1299.

Rodell, M., and J. S. Famiglietti (2001), An analysis of terrestrial water storage variations in Illinois with implications for the Gravity Recovery and Climate Experiment (GRACE), *Water Resour. Res.*, *37*(5), 1327–1339.

Sanchez, E., C. Gallardo, M. A. Gaertner, A. Arribas, and M. Castro (2004), Future climate extreme events in the Mediterranean simulated by a regional climate model: First approach, *Global Planet. Change*, *44*(1–4), 163–180.

Schär, C., D. Lüthi, U. Beyerle, and E. Heise (1999), The soil-precipitation feedback: A process study with a regional climate model, *J. Clim.*, *12*, 722–741.

Schär, C., L. Vasilina, F. Pertziger, and S. Dirren (2004a), Seasonal runoff forecasting using precipitation from meteorological data assimilation systems, *J. Hydrometeorol.*, *5*(5), 959–973.

Schär, C., P. L. Vidale, D. Lüthi, C. Frei, C. Häberli, M. A. Liniger, and C. Appenzeller (2004b), The role of increasing temperature variability in European summer heatwaves, *Nature*, *427*, 332–336, doi:10.1038/nature02300.

Schrodin, R., and E. Heise (2001), The multi-layer version of the DWD soil model TERRA_LM, *Tech. Rep. 2*, Consortium for Small Scale Modeling, Zurich.

Seneviratne, S. I., J. S. Pal, E. A. B. Eltahir, and C. Schär (2002), Summer dryness in a warmer climate: A process study with a regional climate model, *Clim. Dyn.*, *20*(1), 69–85.

Seneviratne, S. I., P. Viterbo, D. Lüthi, and C. Schär (2004), Inferring changes in terrestrial water storage using ERA-40 reanalysis data: The Mississippi river basin, *J. Clim.*, *17*, 2039–2057.

Seneviratne, S. I., et al. (2006a), Soil moisture memory in AGCM simulations: Analysis of Global Land-Atmosphere Coupling Experiment (GLACE) data, *J. Hydrometeorol.*, *7*(5), 1090–1112.

Seneviratne, S. I., D. Lüthi, M. Litschi, and C. Schär (2006b), Land-atmosphere coupling and climate change in Europe, *Nature*, *443*(7108), 205–209.

Steppeler, J., G. Doms, U. Schättler, H. W. Bitzer, A. Gassmann, U. Damrath, and G. Gregoric (2003), Meso-gamma scale forecasts using the nonhydrostatic model LM, *Meteorol. Atmos. Phys.*, *82*, 75–96.

Tapley, B. D., S. Bettadpur, J. C. Ries, P. F. Thompson, and M. M. Watkins (2004), GRACE measurements of mass variability in the Earth system, *Science*, *305*(5683), 503–505.

Taylor, K. E. (2001), Summarizing multiple aspects of model performance in a single diagram, *J. Geophys. Res.*, *106*(D7), 7183–7192.

van den Hurk, B., et al. (2005), Soil control on runoff response to climate change in regional climate model simulations, *J. Clim.*, *18*(17), 3536–3551.

van den Hurk, B. J. J. M., P. Viterbo, A. C. M. Beljaars, and A. K. Betts (2000), Offline validation of the ERA40 surface scheme, *Tech. Memo. 295*, Eur. Cent. for Medium-Range Wather Forecasts, Reading, U. K.

van Ulden, A., G. Lenderink, B. van den Hurk, and E. van Meijgaard (2007), Circulation statistics and climate change in central Europe: PRUDENCE simulations and observations, *Clim. Change*, *81*, suppl. 1, 179–192.

Vidale, P. L., D. Lthi, C. Frei, S. I. Seneviratne, and C. Schr (2003), Predictability and uncertainty in a regional climate model, *J. Geophys. Res.*, *108*(D18), 4586, doi:10.1029/2002JD002810.

Vidale, P. L., D. Lüthi, R. Wegmann, and C. Schär (2007), European summer climate variability in a heterogeneous multi-model ensemble, *Clim. Change*, *81*, suppl. 1, 209–232.

Viterbo, P., and A. C. M. Beljaars (2004), Impact of land surface on weather, in *Vegetation, Water, Humans and the Climate: A New Perspective on an Interactive System*, edited by P. Kabat et al., chap. A.4.5, pp. 52–58, Springer, Berlin.

Wahr, J., S. Swenson, V. Zlotnicki, and I. Velicogna (2004), Time-variable gravity from GRACE: First results, *Geophys. Res. Lett.*, *31*, L11501, doi:10.1029/2004GL019779.

Wetherald, R. T., and S. Manabe (1999), Detectability of summer dryness caused by greenhouse warming, *Clim. Change*, *43*(3), 495–511.

Wetherald, R. T., and S. Manabe (2002), Simulation of hydrologic changes associated with global warming, *J. Geophys. Res.*, *107*(D19), 4379, doi:10.1029/2001JD001195.

Wild, M., A. Ohmura, H. Gilgen, and J.-J. Morcrette (1998), The distribution of solar energy at the Earth's surface as calculated in the ECMWF reanalysis, *Geophys. Res. Lett.*, *25*(23), 4373–4376.

S. Hagemann, Max Planck Institute for Meteorology, Bundesstrasse 55, D-20146 Hamburg, Germany.

M. Hirschi, C. Schär, and S. I. Seneviratne, Institute for Atmospheric and Climate Science, ETH Zurich, Universitaetsstrasse 16, CH-8092 Zurich, Switzerland. (martin.hirschi@env.ethz.ch)